Vibrational predissociation of triatomic van der Waals molecules

J. A. Beswick[a)]

Department of Chemical Physics, The Weizmann Institute of Science, Rehovot, Israel

Joshua Jortner

Department of Chemistry, Tel-Aviv University, Tel Aviv, Israel
(Received 22 August 1977)

In this paper we advance a quantum mechanical colinear model for vibrational predissociation on a single electronic potential surface of a linear triatomic van der Waals molecule X···BC, where BC is a conventional diatomic, while X represents a rare-gas atom. The zero-order states of the system are represented as products of an eigenfunction of the vibrating BC bond and a function describing the (bound or unbound) motion of X relative to the center of mass of BC bond which is frozen at its equilibrium configuration. The residual interaction representing the deviation between the interaction potential of X with the vibrating BC molecule, and the interaction of X with the frozen diatomic, induces discrete–continuum and continuum–continuum coupling. On the basis of the analysis of these coupling terms we assert that the zero-order basis provides a reasonable description of the initial and final states. We have also demonstrated that the zero-order resonance widths are small relative to their spacings and, furthermore, we have shown that continuum–continuum couplings prevail essentially only between adjacent continua. The dynamics of vibrational predissociation were reduced to the problem of the decay of a single resonance into a manifold of adjacently coupled continua. Closed analytical expressions for the rate of vibrational predissociation and for the vibrational distribution of the products were derived incorporating the effects of discrete–continuum and continuum–continuum coupling. We have explored the dependence of the rate of vibrational predissociation on the frequency of the BC molecule establishing a new energy gap law for this process. We have also investigated the dependence of the rate on the potential parameter of van der Waals bond and on the mass of the rare-gas atom. Finally, a study of the nature of the final vibrational distribution of the diatomic fragment resulting from the vibrational predissociation process was provided.

I. INTRODUCTION

Recently, supersonic free expansion has been utilized to prepare a wide variety of weakly bound molecular complexes which involve a rare-gas atom bound to a diatomic or a polyatomic molecule. The recent experimental studies of Klemperer and his colleagues[1] have probed the structural features and the dynamics of nuclear motion of a variety of such van der Waals molecules. Of considerable interest is the nature of intramolecular dynamics of van der Waals molecules in vibrationally excited levels of the ground electronic state and in the electronically excited configurations. An interesting features of excited-state intramolecular relaxation processes in such systems will involve the breaking of weak chemical bonds, which are characterized by bond dissociation energies of the order of 10–200 cm^{-1}. This new class of photofragmentation via vibrational or electronic–vibrational excitation of van der Waals molecules is of considerable experimental and theoretical interest as the (vibrational) excitation energy is relatively low, and optical selection studies of the decay of preselected, individual, vibrational–rotational levels can be conducted. Furthermore, the relevant part of the potential energy surface is relatively simple so that such photofragmentation processes may be amenable to theoretical studies. The photochemical decomposition of vibrationally excited van der Waals molecules on the ground electronic potential surface provides a unique example for vibrational predissociation (VP) of a polyatomic molecule and this nonradiative decay mechanism can also prevail in an electronically excited state of such weakly bound molecular complexes.[2]

Recently, Kim, Smalley, Wharton, and Levy[4] have provided a pioneering study of the photodissociation dynamics of HeI_2, NeI_2, and ArI_2, demonstrating the following:

(a) Photodissociation in the electronically excited $B^3\Pi$ state of HeI_2 occurs via vibrational predissociation.[4(a)]

(b) The VP rate of HeI_2 in the electronically excited state $B^3\Pi$ is $< 5\times10^9$ sec^{-1} for $n=7$ increasing to $\sim 5\times10^{10}$ sec^{-1} for $n=27$, where n is the vibrational quantum number for the I–I stretch.[4(a)]

(c) The VP rate in the $n=1$ level of the ground $X^1\Sigma$ electronic state of HeI_2 is $> 5\times10^6$ sec^{-1}.[4(a)]

(d) The propensity rule $\Delta n=-1$ for VP of HeI_2 in the $B^3\Pi$ state was established.[4(b)]

(e) The occurrence of VP in NeI_2 ($B^3\Pi$) and in high $n>11$ states of $ArI_2(B^3\Pi)$ has been demonstrated.[4(c)]

These results are of great importance as they provide a unique example for VP which is of considerable interest in the elucidation of intramolecular dynamics and unimolecular kinetic processes. In general, the distinction between vibrational predissociation resulting from nuclear motion on a single multidimensional potential surface and electronic predissociation involv-

[a)]Permanent address: Laboratoire de Photophysique Moléculaire, Université de Paris-Sud, Orsay, France.

 0021-9606/78/6805-2277$01.00

ing two electronic configurations is not well defined, and experimental evidence for the former process is sparse. It is therefore not surprising that the interesting area of VP processes was not explored theoretically from the microscopic point of view. The remarkable 1933 paper of Rosen[5] on the mechanism of decomposition of metastable molecules produced by collisions provides a pioneering contribution to this field.

In this paper we present a theoretical study of VP processes in a simple model which involves a linear triatomic van der Waals molecule (VDWM) X···BC, where BC is a normal molecule and X represents a rare-gas atom. Although this model is not directly applicable to the HeI_2 complex, which is characterized by a nonlinear, T-shaped configuration, our theoretical results will be useful in the elucidation of the gross features of the VP processes in some linear van der Waals molecules, such as ArHCl, ArFCl, and also possibly ArI_2, where charge-transfer interaction provides a dominant contribution to the weak bonding. A preliminary report of this work was recently presented.[6] In the present work we provide a detailed account of our model calculations of VP rates for linear triatomic van der Waals molecules. We have explored the dependence of the VP rate on the (high) molecular frequency of B–C, on the binding energy and the mass of the rare-gas atom, and on the (low) B–X vibrational frequency, as well as the nature of the final vibrational distribution of the product BC resulting from the VP process.

II. POTENTIAL SURFACES AND ZERO-ORDER STATES

We consider a triatomic VDWM X···BC restricted to one-dimensional motion on a simple adiabatic potential energy surface which is approximated by the superposition of the B–C intermolecular potential and the X···B van der Waals interaction

$$V(R_{XB}, R_{BC}) = V_{XB}(R_{XB}) + V_{BC}(R_{BC}) \ . \tag{1}$$

The two terms in Eq. (1) depend on the interatomic distances between adjacent atoms R_{XB} and R_{BC}, respectively. The intramolecular potential for the normal BC bond will be characterized either in terms of a harmonic potential

$$V_{BC}(R_{BC}) = (1/2)k_{BC}(R_{BC} - \bar{R}_{BC})^2 \tag{2a}$$

or by a Morse potential

$$V_{BC}(R_{BC}) = D_{BC}\{\exp[-2\alpha_{BC}(R_{BC} - \bar{R}_{BC})] - 2\exp[-\alpha_{BC}(R_{BC} - \bar{R}_{BC})]\} \ , \tag{2b}$$

where $\bar{R}_{BC}$ is the bond equilibrium distance, D_{BC} is the bond dissociation energy, k_{BC} is the force constant for the harmonic oscillator, while α_{BC} is the characteristic inverse length for the Morse oscillator. The latter two quantities are related to the frequency $\omega_{BC} = [(\partial^2 V_{BC}/\partial R_{BC}^2)/\mu_{BC}]^{1/2}_{\bar{R}_{BC}}$, where $\mu_{BC} = m_B m_C/(m_B + m_C)$ is the reduced mass, via $k_{BC} = \mu_{BC}\omega_{BC}^2$ for the harmonic case and $\alpha_{BC} = \omega_{BC}(\mu_{BC}/2D_{BC})^{1/2}$ for the Morse potential. The theory of VP will be applied for both forms of the B–C potential to assess the effects of intramolecular anharmonicity on this process. The van der Waals interaction V_{XB} was specified in terms of a Morse potential

$$V_{XB}(R_{XB}) = D_{XB}\{\exp[-2\alpha_{XB}(R_{XB} - \bar{R}_{XB}) - 2\exp[-\alpha_{XB}(R_{XB} - \bar{R}_{XB})]\} \ , \tag{3}$$

where D_{XB} and $\bar{R}_{XB}$ are the minimum energy and the equilibrium distance, respectively. We can define an effective frequency ω_{XB} for the van der Waals bond $\omega_{XB} = [(\partial^2 V_{XB}/\partial R_{XB}^2)/\mu_{X,BC}]^{1/2}_{\bar{R}_{XB}}$, where $\mu_{X,BC} = m_X(m_B + m_C)/(m_X + m_B + m_C)$ is the reduced mass for the X···BC motion. The characteristic inverse length for the van der Waals bond can be expressed as $\alpha_{XB} = \omega_{XB}(\mu_{X,BC}/2D_{XB})^{1/2}$. The currently available data concerning the potential parameters characterizing the van der Waals bond are sparse. The following information was utilized:

(1) Secrest and Eastes[7] have compiled some semiempirical Lennard-Jones (LJ) potential parameters for the interaction of rare-gas atoms with a variety of diatomics, their potential being represented in the familiar form

$$V_{XB}(R_{XB}) = d_{XB}[(r_0/R_{XB})^{12} - 2(r_0/R_{XB})^6] \ . \tag{4}$$

To extract the Morse potential parameters [Eq. (3)] from the LJ potential parameters [Eq. (4)] we use the following relations: $D_{XB} = d_{XB}$, $\bar{R}_{XB} = r_0$, and $\alpha_{XB} = 6/r_0$. The last relation originates from taking the values of $(\partial^2 V_{XB}/\partial R_{XB}^2)_{\bar{R}_{XB}}$ obtained for both potentials (3) and (4) to be equal. The resulting Morse potential parameters thus obtained from the data presented by Secrest and Eastes[7] are summarized in Table I.

(2) Novick *et al.*[1(a)] have derived a nonharmonic trial potential for linear ArHCl and ArDCl. The angularly averaged potential for these systems is characterized by $\bar{R}_{XB} \simeq 3.9$ Å and $D_{XB} \simeq 160$ cm^{-1}, in reasonable agreement with the semiempirical Morse potential parameters derived from the data of Secrest and Eastes.[7]

(3) Smalley and colleagues[4(b)] have observed a vibrational structure in the electronic absorption spectrum transitions to the $l = 0$ and $l = 1$ vibrational states of the He···I_2 mode. The HeI_2 molecule is not linear but rather T-shaped with a distance of ~4 Å from the He to the center of the I_2 bond.[4(c)] Levy *et al.*[4(c)] have conducted a rough estimate of the He···I_2 binding energy. Assuming a perpendicular motion of the rare-gas atom with respect to the I–I bond the energy separation ΔE_{10} between the $l = 1$ and $l = 0$ vibrational states can be expressed as $\Delta E_{10} = \hbar\omega_{XB}(1 - K_{XB}^{-1})$, where $K_{XB} = 2D_{XB}/\hbar\omega_{XB}$ determines the number of bound levels [actually the number of bound levels supported by a Morse potential is given by N = integer $(K_{XB} + \frac{1}{2})$]. Kim, Smalley, Wharton, and Levy have reported the value of $\Delta E_{10} = 6$ cm^{-1} for the $B^3\Pi$ configuration of HeI_2. Taking the parameter K_{XB} to be $K_{XB} = 1.5$ corresponding to two bound vibrational states of the VDWM the relations above yields $\omega_{XB} = 18$ cm^{-1}, $D_{XB} = 13.5$ cm^{-1}, which results in the reasonable value $\alpha_{XB} = 1.18$ Å^{-1}.

We now proceed to describe the nuclear dynamics on a single potential surface. One possible set of coordinates (see however Ref. 5 and Appendix B) appropriate for this linear VP problem of a triatomic

TABLE I. Compilation of Morse potential parameters for some van der Waals bonds between rare-gas atoms and diatomic molecules.

Molecule	D_{XB} (cm^{-1})	$\bar{R}_{XB}$ (Å)	α_{XB} ($Å^{-1}$)	ω_{XB} (cm^{-1})	Number of bound states	ΔE_{01} (cm^{-1})	Reference	Molecular configuration
HeI_2	52.	4.24	1.42	42.4	2	25.1	7	T shaped
	13.5	~4.	1.18	18.	2	6.	3(b)	
NeI_2	97.4	4.36	1.38	26.	7	22.5	7	
ArI_2	181.5	4.71	1.27	24.	15	22.4	7	
ArHCl	130.	4.4	1.36	30.	9	26.5	7	
	160.	3.9	1.54	36.7	9	32.5	1(a)	Linear

Useful formulas for Morse potentials:

$V(R)=D\{\exp[-2\alpha(R-\bar{R})]-2\exp[-\alpha(R-\bar{R})]\}$, $H=-(\hbar^2/2\mu)d^2/\partial R^2+V(R)$,

$\omega=\mu^{-1}(d^2V/dR^2)_{\bar{R}}=\alpha(2D/\mu)^{1/2}$.

Number of bound states = integer $(\kappa+\frac{1}{2})$ with $\kappa=2D/\hbar\omega$

Energy of bound states:

$W_l=-(\hbar\omega/2\kappa)(\kappa-l-\frac{1}{2})^2$, $l=0,1,\ldots,$ integer $(\kappa-\frac{1}{2})$,

$=-D+\hbar\omega(l+\frac{1}{2})-\chi(l+\frac{1}{2})^2$; $\chi=1/2\kappa$,

$\Delta_{01}=E_1-E_0=\hbar\omega(1-1/\kappa)$.

VDWM involves the center of mass coordinate of the entire system, the interatomic distance R_{BC} of the conventional molecule BC, and the distance $R_{X,BC}$ between the atom X and the center of mass of the molecular fragment BC:

$$R_{X,BC}=R_{XB}+\gamma R_{BC}\,,\quad \gamma=m_C/(m_B+m_C)\,. \tag{5}$$

The Hamiltonian for the internal motion, obtained after the separation of the center of mass motion of the whole system, assumes the form

$$H=-(\hbar^2/2\mu_{X,BC})\partial^2/\partial R_{X,BC}^2 - (\hbar^2/2\mu_{BC})\partial^2/\partial R_{BC}^2+V_{BC}(R_{BC})+V_{XB}(R_{X,BC}-\gamma R_{BC})\,. \tag{6}$$

The Hamiltonian (6) will now be segregated in the following manner:

$$H=H_0+\upsilon\,, \tag{7}$$

the zero-order Hamiltonian H_0 being

$$H_0=H_{BC}+H_{X,BC}\,, \tag{7a}$$

$$H_{BC}=-(\hbar^2/2\mu_{BC})\partial^2/\partial R_{BC}^2+V_{BC}(R_{BC})\,,$$

$$H_{X,BC}=-(\hbar^2/2\mu_{X,BC})\partial^2/\partial R_{X,BC}^2+V_{XB}(R_{X,BC}-\gamma\bar{R}_{BC})\,,$$

while the residual perturbation term is

$$\upsilon=V_{XB}(R_{X,BC}-\gamma R_{BC})-V_{XB}(R_{X,BC}-\gamma\bar{R}_{BC})\,. \tag{7b}$$

The zero-order Hamiltonian (7a) corresponds to separable contributions from a vibrating BC bond and from the motion of X relative to the center of mass of the BC bond which is now frozen at its equilibrium distance $\bar{R}_{BC}$.

We shall now construct the zero-order "nuclear diabatic" solutions for the zero-order Hamiltonian (7a). These consist of (a) discrete, bound, vibrational states of the VDWM

$$|nl\rangle=\chi_n(R_{BC})\phi_l(R_{X,BC})\,, \tag{8}$$

where n denotes the discrete vibrational number of the BC molecular bond, while l corresponds to the discrete vibrational quantum number of the van der Waals bond; these bound states are characterized by the energies $E_{nl}=W_n+W_l$, where W_n and W_l correspond to the energies of the discrete levels χ_n and ϕ_l, respectively; (b) continuum states of the fragments X + BC

$$|n\epsilon\rangle=\chi_n(R_{BC})\phi_\epsilon(R_{X,BC})\,, \tag{9}$$

where n denotes again the vibrational quantum number for the BC molecular bond and ϵ designates the relative kinetic energy between X and BC. The continuum states are energy normalized, being characterized by the energies $E_{n\epsilon}=W_n+\epsilon$.

The zero-order nuclear diabatic states are coupled by υ [Eq. (7b)]; the relevant discrete–discrete (d–d), discrete–continuum (d–c), and continuum–continuum (c–c) coupling terms are, respectively,

$$V^{d-d}=\hat{P}\upsilon\hat{P}\,,\quad V^{d-c}=\hat{P}\upsilon\hat{Q}\,,\quad V^{c-c}=\hat{Q}\upsilon\hat{Q}\,, \tag{10a}$$

$$\hat{P}=\sum_n\sum_l |nl\rangle\langle nl|\,,\quad \hat{Q}=\sum_n\int d\epsilon\,|n\epsilon\rangle\langle n\epsilon|\,. \tag{10b}$$

These coupling matrix elements $V^{a-b}_{n\alpha,n'\beta}\equiv\langle n\alpha|V^{a-b}|n'\beta\rangle$ (where $a,\ b\equiv d,\ c$; $\alpha,\ \beta\equiv l,\ \epsilon$) were evaluated in an analytic form for the potentials (1), (2a), and (3) and for the potentials (1), (2b), and (3). Details of the calculation are presented in Appendix A. The discrete–discrete coupling terms will turn out to be of minor interest. The discrete–continuum coupling terms (10a) take the form

$$V^{d-c}_{nl,n'\epsilon}=(A^{(2)}_{nn'}B^{(2)}_{l\epsilon}-2A^{(1)}_{nn'}B^{(1)}_{l\epsilon})\,, \tag{11}$$

where

$$A^{(j)}_{nn'} = \int_{-\infty}^{\infty} \chi_n(R_{BC})\{\exp[j\alpha_{XB}\gamma(R_{BC}-\bar{R}_{BC})]-1\} \times \chi_{n'}(R_{BC})\,dR_{BC} \quad (j=1,\,2)\,, \tag{12}$$

$$B^{(1)}_{l\epsilon} = (1/2)\left[(D_{XB}/2)\sin(2\pi\theta_\epsilon)\,\frac{(2K_{XB}-2l-1)}{l!\,\Gamma(2K_{XB}-l)}\right]^{1/2} \times \frac{|\Gamma(1/2+K_{XB}-i\theta_\epsilon)|}{[\cos^2(\pi K_{XB})+\sinh^2(\pi\theta_\epsilon)]^{1/2}}\,, \tag{13a}$$

$$B^{(2)}_{l\epsilon} = (B^{(1)}_{l\epsilon}/2K_{XB})[(K_{XB}-l-1/2)^2+\theta_\epsilon^2+2K_{XB}]\,, \tag{13b}$$

with the definitions

$$K_{XB} = (\hbar\alpha_{XB})^{-1}(2\mu_{X,BC}D_{XB})^{1/2} \equiv 2D_{XB}/\hbar\omega_{XB}\,, \tag{13c}$$

$$\theta_\epsilon = (\hbar\alpha_{XB})^{-1}(2\mu_{X,BC}\epsilon)^{1/2} \equiv 2(D_{XB}\epsilon)^{1/2}/\hbar\omega_{XB}\,, \tag{13d}$$

and where $\Gamma(Z)$ stands for the gamma function of a complex argument. The integrals $A^{(2)}_{nn'}$ and $A^{(1)}_{nn'}$ for the harmonic bond [Eq. (2a)] were given by Rapp and Sharp[8] as

$$A^{(j)}_{nn'} = (n!/n'!)^{1/2}\,\beta_j^{n'-n}\exp(\beta_j^2/2)L_n^{n'-n}(-\beta_j^2) \quad (j=1,\,2)\,, \tag{14a}$$

where $\beta_j = j\hbar\alpha_{BC}\gamma/(2\mu_{BC}\hbar\omega_{BC})^{1/2}$ and $L_n^{n'-n}$ is the generalized Laguerre polynomial, while for the Morse potential [Eq. (2b)] these are given by[9]

$$A^{(j)}_{nn'} = -\delta_{mm'} + \left[\frac{(n')!\,(2K_{BC}-2n'-1)(2K_{BC}-2n-1)}{n!\,\Gamma(2K_{BC}-n)}\,\Gamma(2K_{BC}-n')\right]^{1/2} \times (2K_{BC})^{(j\alpha_{XB}\gamma/\alpha_{BC})} \sum_{m=0}^{n'}(-1)^m\,\frac{\Gamma(n-j\alpha_{XB}\gamma/\alpha_{BC}-m)\Gamma(-n-j\alpha_{XB}\gamma/\alpha_{BC}-m+2K_{BC}-1)}{m!\,(n'-m)!\,\Gamma(2K_{BC}-n'-m)\Gamma(-j\alpha_{XB}\gamma/\alpha_{BC}-m)} \tag{14b}$$

for $j=1,\,2$ and $n \geq n'$, with the definition $K_{BC} = (\hbar\alpha_{BC})^{-1}(2\mu_{BC}D_{BC})^{1/2}$. The continuum–continuum couplings [Eq. (10a)] take the final form

$$V^{c-c}_{n'\epsilon',n\epsilon} = (A^{(2)}_{n'n}B^{(2)}_{\epsilon'\epsilon} - 2A^{(1)}_{n'n}B^{(1)}_{\epsilon'\epsilon})\,, \tag{15}$$

with

$$B^{(1)}_{\epsilon'\epsilon} = (K_{XB}/2)\,|\Gamma(1/2-K_{XB}-i\theta_\epsilon)\Gamma(1/2-K_{XB}-i\theta_{\epsilon'})| \times \frac{[\sinh(2\pi\theta_\epsilon)\sinh(2\pi\theta_{\epsilon'})]^{1/2}}{\cosh(2\pi\theta_\epsilon)-\cosh(2\pi\theta_{\epsilon'})}\,[\,|\Gamma(1/2-K_{XB}-i\theta_\epsilon)|^{-2}-|\Gamma(1/2-K_{XB}-i\theta_{\epsilon'})|^{-2}]\,, \tag{16a}$$

$$B^{(2)}_{\epsilon'\epsilon} = (1/4)\,|\Gamma(1/2-K_{XB}-i\theta_\epsilon)\Gamma(1/2-K_{XB}-i\theta_{\epsilon'})| \times \frac{[\sinh(2\pi\theta_\epsilon)\sinh(2\pi\theta_{\epsilon'})]^{1/2}}{\cosh(2\pi\theta_\epsilon)-\cosh(2\pi\theta_{\epsilon'})}\left[\frac{\theta_\epsilon^2-\theta_{\epsilon'}^2+2K_{XB}}{|\Gamma(1/2-K_{XB}-i\theta_\epsilon)|^2}+\frac{\theta_\epsilon^2-\theta_{\epsilon'}^2-2K_{XB}}{|\Gamma(1/2-K_{XB}-i\theta_{\epsilon'})|^2}\right]\,, \tag{16b}$$

where K_{XB} and θ_ϵ are defined in terms of Eqs. (13c) and (13d), respectively. Equation (15) is closely related to Devonshire's results.[10]

In Fig. 1 we portray the spectrum of the zero-order Hamiltonian [Eq. (7a)] together with the relevant coupling terms. Extensive numerical studies of the d–d coupling [Eqs. (A8a) and (A8b)], of the d–c coupling [Eqs. (11)–(14)], and of the c–c coupling [Eqs. (14)–(16)] were conducted by us. From these numerical calculations some general characteristics emerge which will considerably simplify the treatment of the VP prob-

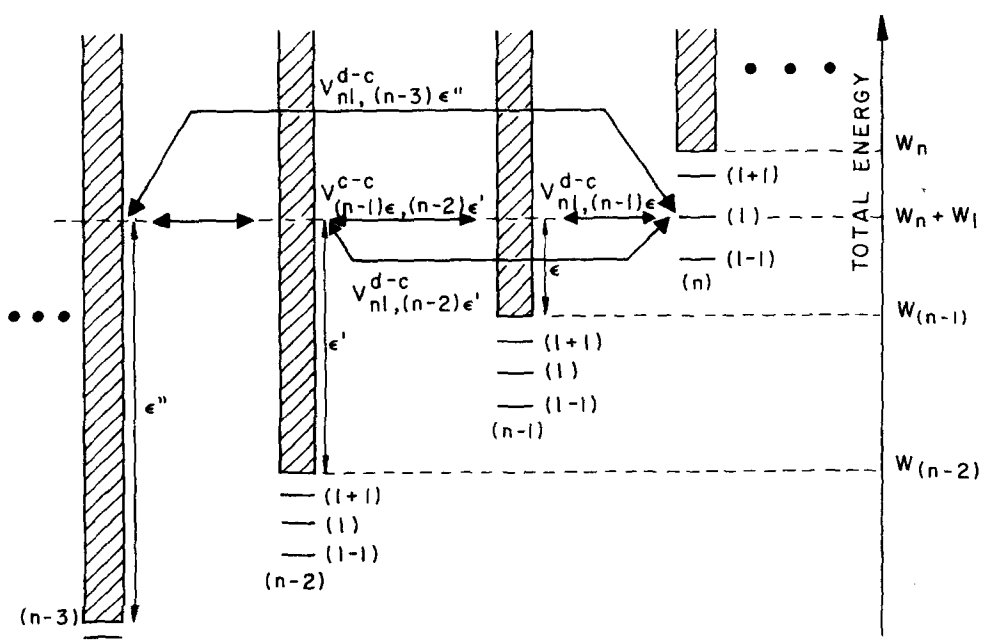

FIG. 1. Spectrum of the zero-order Hamiltonian and relevant coupling terms appropriate for the description of vibrational predissociation of a van der Waals molecule X···BC, where X is a rare-gas atom and BC a conventional diatomic molecule. The system is initially in the discrete level $|n,l\rangle$ with zero-order energy W_n+W_l, where n is the quantum number associated with the vibration of the BC molecule and l is the quantum number associated with the bound motion of X with respect to BC.

TABLE II. Discrete–discrete coupling terms between neighboring levels calculated for model linear VDWM. The molecular bond BC is characterized by the following parameter: $D_{BC} = 4911$ cm^{-1}, $\omega_{BC} = 128$ cm^{-1} for $I_2(B\,^3\Pi)$.

Molecule	Molecular parameters	$(n,l) \rightarrow (n'l')$	$E_{n'l'} - E_{nl}$ (cm^{-1})	$V^{d-d}_{nl,n'l'}$ (cm^{-1})
HeI_2	$D_{XB} = 14$ cm^{-1}	$(0,0) \rightarrow (0,1)$	6.4	0.53×10^{-2}
		$(5,0) \rightarrow (5,1)$	6.4	0.66×10^{-1}
	$\omega_{XB} = 18$ cm^{-1}	$(10,0) \rightarrow (10,1)$	6.4	0.14
		$(20,0) \rightarrow (20,1)$	6.4	0.37
	$D_{XB} = 50$ cm^{-1}	$(0,0) \rightarrow (0,1)$	24.4	0.98×10^{-1}
		$(5,0) \rightarrow (5,1)$	24.4	1.21
	$\omega_{XB} = 42$ cm^{-1}	$(10,0) \rightarrow (10,1)$	24.4	2.63
		$(20,0) \rightarrow (20,1)$	24.4	6.88
NeI_2	$D_{XB} = 100$ cm^{-1}	$(0,0) \rightarrow (0,1)$	22.6	0.21
		$(0,2) \rightarrow (0,3)$	15.9	0.20
		$(0,4) \rightarrow (0,5)$	9.1	0.1
		$(0,6) \rightarrow (0,7)$	2.3	0.11×10^{-1}
	$\omega_{XB} = 26$ cm^{-1}	$(10,0) \rightarrow (10,1)$	22.62	5.58
		$(10,2) \rightarrow (10,3)$	15.9	5.42
		$(10,4) \rightarrow (10,5)$	9.1	2.85
		$(10,6) \rightarrow (10,7)$	2.34	0.33
NeI_2		$(20,0) \rightarrow (20,1)$	22.6	14.16
		$(20,2) \rightarrow (20,3)$	15.9	14.
		$(20,4) \rightarrow (20,5)$	9.1	7.6
		$(20,6) \rightarrow (20,7)$	2.3	0.96
ArI_2	$D_{XB} = 180$ cm^{-1}	$(0,0) \rightarrow (0,1)$	22.4	0.28
		$(0,4) \rightarrow (0,5)$	16.	0.36
		$(0,8) \rightarrow (0,9)$	9.6	0.21
		$(0,12) \rightarrow (0,13)$	3.2	0.42×10^{-1}
	$\omega_{XB} = 24$ cm^{-1}	$(10,0) \rightarrow (10,1)$	22.4	7.38
		$(10,4) \rightarrow (10,5)$	16.	9.54
		$(10,8) \rightarrow (10,9)$	9.6	5.6
		$(10,12) \rightarrow (10,13)$	3.2	1.23
		$(20,0) \rightarrow (20,1)$	22.4	18.4
		$(20,4) \rightarrow (20,5)$	16.	24.2
		$(20,8) \rightarrow (20,9)$	9.6	14.6
		$(20,12) \rightarrow (20,13)$	3.2	3.5

[a]Obtained from the values of ω_l and $\omega_l\chi_l$ given in Ref. 17, by using the formulas of Table I.

lem. The main features of the coupling terms are the following:

(a) The discrete–discrete coupling terms [Eqs. (A8a) and (A8b)] are usually small relative to the energy spacing between the discrete levels. In Table II we present some numerical results which demonstrate this point. From these numerical data it is apparent that

$$|E_{nl} - E_{n'l'}| \gg |V^{d-d}_{nl,n'l'}| \tag{17}$$

for most of the cases. This result clearly demonstrates that at least for low n the shifts of the discrete levels due to the d–d coupling are small.

(b) The dominant contributions to the continuum–continuum coupling originate from those terms where $\Delta n = \pm 1$. For the harmonic potential description of the BC bond [Eq. (2a)] the $V^{c-c}_{n\epsilon,n'\epsilon'}$ terms identically vanish for $\Delta n \neq \pm 1$ if the exponential in Eq. (12) is expanded in α_{XB} and only the linear term is retained. For the case of a Morse type BC potential we have conducted numerical studies of the c–c coupling, a sample of our results is portrayed in Fig. 2 for on-the-energy-shell c–c coupling terms, at the energy of a discrete level (n, l). We denote by $V^{c-c}_{n',n''}$ the matrix element $V^{c-c}_{n'\epsilon',n''\epsilon''}$ with the condition that $W_{n'} + \epsilon' = W_{n''} + \epsilon'' = W_n + W_l$. From this figure it is apparent that $V^{c-c}_{n',n''}$ decreases very fast with decreasing n'' and that $V^{c-c}_{n',n'-1}$ is the dominating c–c coupling term. We shall accordingly set

$$V^{c-c}_{n',n''} = V^{c-c}_{n',n'-1}\,\delta_{n',n''+1}\,, \quad n' > n''\,, \tag{18}$$

disregarding c–c coupling for $\Delta n \neq \pm 1$.

(c) The discrete–continuum coupling terms $V^{d-c}_{nl,n'\epsilon}$ $\times (n' < n)$ evaluated on the energy shell (i.e., $W_n + W_l = W_{n'} + \epsilon$) are dominated by the term $n - n' = 1$. Again, as for the case of c–c coupling, Fig. 2 shows that the d–c coupling $V^{d-c}_{nl,n'\epsilon}$ decreases very fast with decreasing n'.

(d) In many cases of interest for physically acceptable energetic parameters of the VDWM we found that the square of the modulus of the discrete–continuum coupling terms $|V^{d-c}_{nl,n'\epsilon}|^2$ (which are given in units of energy are appreciably smaller than the energy spacing between the discrete levels, i.e.,

$$|V^{d-c}_{nl,n'\epsilon}|^2 \ll |E_{n''l''} - E_{n'l'}| \tag{19}$$

for all $|n'l'\rangle$ and $|n''l''\rangle$.

(e) To assess the effects of the anharmonicity of the BC bond on the various coupling terms several observations are in order. First, concerning the d–c coupling terms $V^{d-c}_{nl,(n-1)\epsilon}$ we note (see Fig. 3) that for moderately low values of $n(\leq 5)$ the effect of the anharmonicity of the BC bond is small. However, at higher values of n the anharmonicity of the molecular bond considerably enhances the d–c coupling relative to the harmonic case. Thus, as we shall see in Sec. IV, the anharmonicity of the BC molecule results in a quantitative modification of the dynamics of VP. Second, the c–c coupling $V^{c-c}_{n',n'-1}$ terms are also modified by anharmonicity effects, in particular for large values of n [see Figs. 4(a) and 4(b)]. It is instructive to note that the harmonic potential overestimates in many cases the c–c coupling between adjacent continua and the effects of anharmonicity of the molecular bond tend to reduce the relevant intercontinuum coupling terms.

III. MODEL FOR VIBRATIONAL PREDISSOCIATION

On the basis of the foregoing discussion of the general characteristics of the coupling terms we shall now invoke the following simplifying assumptions which will underline our treatment of the VP problem:

(1) Discrete–discrete interactions will be neglected according to Eq. (17).

(2) Continuum–continuum coupling interactions for $\Delta n \neq \pm 1$ will be neglected according to Eq. (18).

(3) The zero-order widths of the resonances $\pi|V^{d-c}_{nl,n'\epsilon}|^2$, originating from discrete–continuum coupling, are assumed to be small relative to the energy spacing between the discrete levels, as asserted by Eq. (18). Thus, in the treatment of the decay problem interference effects between resonances can be disregarded.

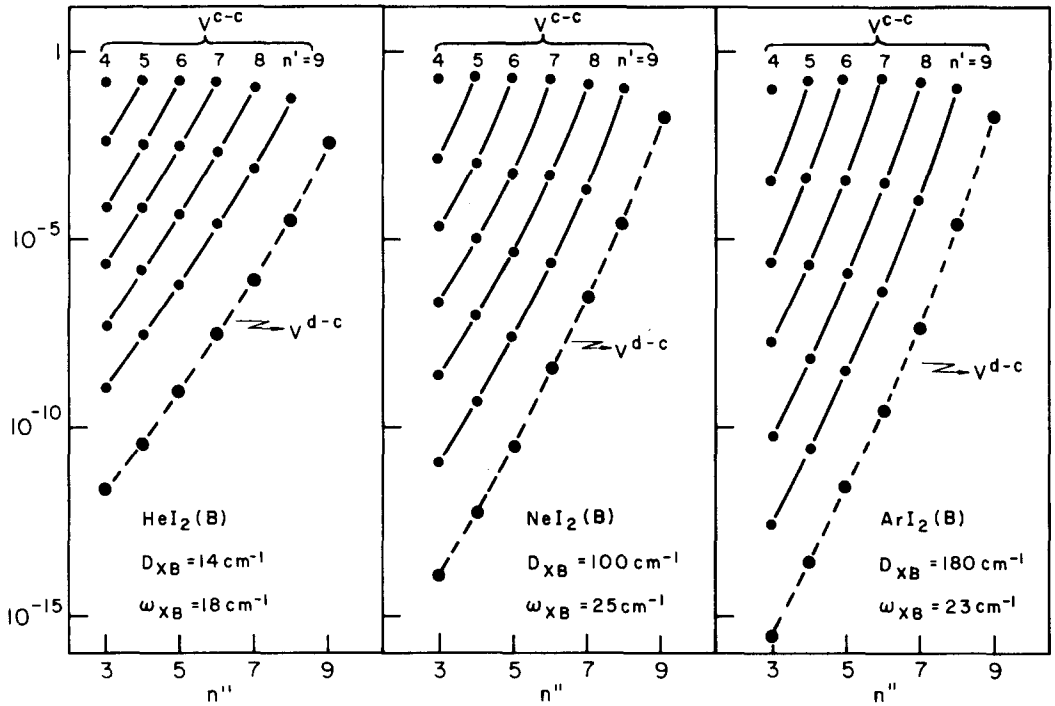

FIG. 2. On-the-energy-shell continuum-continuum V^{c-c} and discrete–continuum V^{d-c} couplings involved in the predissociation of some model $XI_2(B)$, X≡He, Ne, Ar, from level $n=10$ [n being the quantum number of the $I_2(B)$ molecule]. The points connected by solid lines correspond to the continuum–continuum couplings $V^{c-c}_{n',n''}$ where n' is specified on top of each line and n'' is marked on the abscissa. The points connected by dashed lines correspond to the discrete–continuum coupling $|V^{d-c}_{10,n''}|/(\hbar\omega_{I_2})^{1/2}$. Note that with these definitions all the couplings are adimensional. The I–I bond in the $B\,^3\Pi$ state was specified in terms of an anharmonic potential with paramteres taken from Ref. 17. The parameters for the van der Waals interaction between X and the $I_2(B)$ molecule are marked on the figure (see also Table I).

These points pertain to the description of the energy levels. An additional assumption has to be invoked to specify the "preparation" of the vibrationally excited state or the electronically–vibrationally excited state of the VDWM which undergoes VP.

(4) Only the discrete zero-order excited states carry oscillator strength from the ground state[11] $|g;\ n=0,\ l=0\rangle$, where g refers here to the ground state electronic wavefunction. The optical excitation of the VDWM can be adequately described in terms of the radiative coupling $|g;\ n=0,\ l=0\rangle \rightarrow |g;\ n'l'\rangle$ $(n'\neq n)$ between zero-order discrete levels for infrared excitation or by $|g;\ n=0,\ l=0\rangle \rightarrow |s;\ n'l'\rangle$ for electronic–vibrational excitation, where $|s\rangle$ represents a higher electronic configuration. The transition moments to the continuum states which correspond to the radiative couplings $|g;\ n=0,\ l=0\rangle \rightarrow |g;\ n'\epsilon\rangle$ or $|g;\ n=0,\ l=0\rangle \rightarrow |s;\ n'\epsilon\rangle$ are assumed to be negligibly small. For example, in the case of electronic–vibrational excitation we expect that the transition moment in the Condon approximation $|\mu_{gs}|^2|\langle n=0|n'\rangle|^2|\langle l=0|l'\rangle|^2$, where $\mu_{gs}=\langle s|\mu|g\rangle$ corresponds to the electronic matrix element of the dipole moment operator, will be largest for $l'=l$ and that the nuclear vibrational overlap $|\langle l=0|\epsilon\rangle|^2$ will be very small. This expectation is borne out by the spectroscopic data of Smalley *et al.*[4(a),4(b)] on HeI_2 which indicate that the electronic–vibrational transition moment from $|X'\Sigma;\ n=0,\ l=0\rangle$ to the $|B^3\Pi;\ n'l=0\rangle$ state is by 1–2 orders of magnitude larger than the transition moment to the $|B^3\Pi;\ n'l=1\rangle$ state and no evidence for Fano type resonances,[12] which will indicate that the (zero-order) continuum states carry appreciable oscillator strength, is exhibited.

On the basis of assumptions (1) and (3) we can assert that the nuclear diabatic zero-order basis set provides a reasonable description of the energy levels of the real system as level shifts due to discrete–discrete and discrete–continuum off-resonance interactions are expected to be small. On the basis of assumption (4) we can subsequently consider the decay of "initially prepared" discrete states for a proper description of the VP dynamics, as is common in the treatment of electronic relaxation and predissociation processes.[13] A more elaborate formal treatment of the "preparation" problem can be provided following the technique introduced by Mukamel for the study of electronic predissociation.[13] Focusing attention again on assumption (3) we can limit ourselves to the treatment of the decay of a single discrete zero-order state into a manifold of dissociative zero-order continua which are coupled among themselves. Finally, assumption (2) results in a considerable technical simplification of the continuum–continuum coupling problem as we can consider only the coupling between adjacent continua.

The physical picture of VP rests on a definition of a physically reasonable zero-order nuclear diabatic basis and the residual interaction [Eq. (7b)] representing the deviation between the interaction potential of the rare-gas atom interacting with the vibrating diatomic, and the interaction potential between X and BC, which is frozen

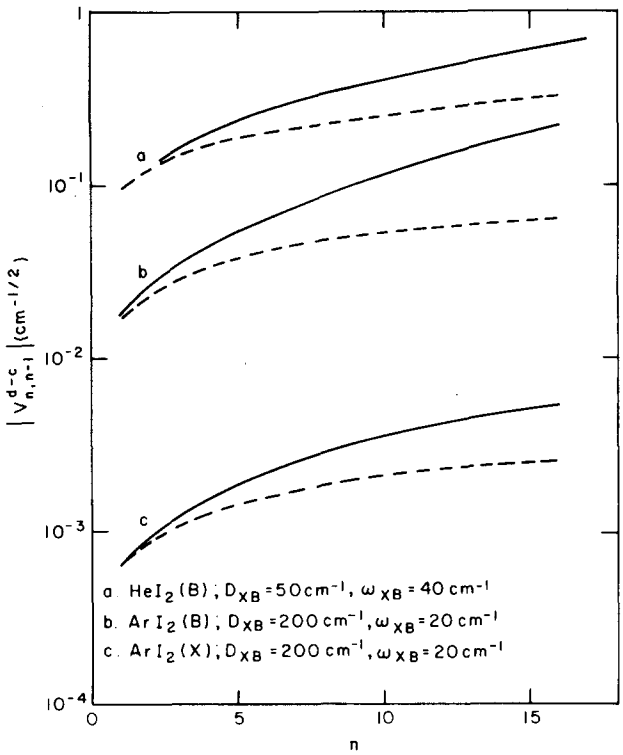

FIG. 3. Effect of the anharmonicity on the discrete–continuum couplings for the VP of some model linear van der Waals molecules. The initial discrete state is specified by the quantum numbers (n,l), where n is marked on the abscissa, while $l=0$ for curve (a), $l=9$ for curve (b), and $l=13$ for curve (c). The figure portrays on-the-energy-shell discrete–continuum coupling $|V^{d-c}_{n,n-1}|$ for an I–I bond represented by a harmonic potential (dashed curve), or an anharmonic potential (solid curve) with parameters taken from Ref. 17. The parameters for the van der Waals interaction between X and I_2 molecule are marked on the figure (see also Table I).

at its equilibrium nuclear separation, induces discrete–continuum and continuum–continuum resonance couplings. These coupling terms will determine the dynamics of the (physically acceptable) initially prepared discrete state $|nl\rangle$ which undergoes VP. We note in passing that the representation of the zero-order states and the residual coupling in terms of a picture, which bears a close analogy to the distorted wave description in molecular scattering,[14] is not unique. An alternative description can be obtained for the linear VDWM in terms of Rosen's relative coordinate treatment[5] where a kinetic energy term provides the residual coupling (see Appendix B).

Figure 5 presents the simplified level scheme appropriate for the treatment of VP of a VDWM. The VP problem now reduces to the decay of a single discrete zero-order state $|nl\rangle$ into a manifold of adjacently coupled continua.[15] Invoking the initial condition $\Psi(t=0) = |nl\rangle$ the probability $P_{n'}(t)$ to be in the n' continuum is given by

$$P_{n'}(t) = \int d\epsilon \, |\langle n'\epsilon | \hat{U}(t,0) | nl\rangle|^2 \tag{20}$$

where $\hat{U}(t) = \exp(-iHt/\hbar)$ is the time evolution operator. The final probability distribution of the fragments among the various vibrational channels is

$$P_{n'} = P_{n'}(\infty) , \tag{21}$$

while the decay probability of the initial state is

$$p^{nl}(t) = |\langle nl | \hat{U}(t,0) | nl\rangle|^2 . \tag{22}$$

Utilization of resolvent operator methods, together with the first-order K matrix approximation which neglects level shift contributions to the transition operator on the dissociative potential surface, results in explicit expressions for the decay and population probabilities.[15] This approach amounts essentially to neglecting the weak energy dependence of the $d-c$ and $c-c$ coupling as well as the effect of thresholds of the dissociative continua. Following our previous work[15] (see Appendix C) the probability for VP [Eq. (22)] assumes the exponential decay law

$$p^{nl}(t) = \exp(-2\Gamma_{nl}\, t/\hbar) , \tag{23}$$

where the total decay rate $\omega_{nl} = (2\Gamma_{nl}/\hbar)$, the decay half-width being

$$\Gamma_{nl} = \pi \, \mathrm{Re}\left[\sum_{n'} \sum_{n''} V^{d-c}_{nl,n''} F(n', n'') V^{d-c}_{n'',nl}\right] , \tag{24}$$

where $V^{d-c}_{nl,n''}$ denotes the coupling between $|nl\rangle$ and the continuum states $|n''\epsilon''\rangle$ on the energy shell, i.e., $\omega_n + \omega_l = \omega_{n''} + \epsilon''$. $F(n', n'') = \langle n'\epsilon' | \hat{F} | n''\epsilon''\rangle$ are the matrix elements of the wave operator

$$\hat{F} = (1 + i\pi \hat{V}^{c-c})^{-1} \tag{25}$$

evaluated on the energy shell, i.e., $\omega_n + \omega_l + \omega_{n'} + \epsilon' = \omega_{n''} + \epsilon''$. The time dependence of a population of a given dissociative channel [Eq. (20)] is

$$P_{n'}(t) = (\pi/\Gamma_{nl}) \left| \sum_{n''} F(n', n'') V^{d-c}_{n'',nl} \right|^2 [1 - \exp(-2\Gamma_{nl}\, t/\hbar)] , \tag{26}$$

while the final branching ratio among vibrational channels is

$$P_{n'} = (\pi/\Gamma_{nl}) \left| \sum_{n''} F(n', n'') V^{d-c}_{n'',nl} \right|^2 . \tag{27}$$

Thus, the dynamics of VP is now determined by the $d-c$ coupling terms and the wave operator, which is determined by the $c-c$ coupling. In the case of couplings only between adjacent continua the $\hat{F}$ matrix can be expressed in the form[15]

$$F(n', n'') = \frac{Q_\alpha \bar{Q}_\beta}{Q_n} \prod_{j=\alpha}^{\beta-1} (-i\pi V^{c-c}_{j,j+1}) , \tag{28}$$

where, as before, $V^{c-c}_{j,j+1}$ denotes the coupling between two adjacent continua on the energy shell of the initial discrete state $|nl\rangle$, $\alpha = \min(n', n'')$, $\beta = \max(n', n'')$ and Q_α and $\bar{Q}_\beta$ are polynomials determined by the recurrence relations

$$Q_0 = Q_1 = 1 ,$$

$$Q_{j+1} = Q_j + \pi^2 |V^{c-c}_{j-1,j}|^2 Q_{j-1} , \tag{29a}$$

and

$$\bar{Q}_{n-1} = \bar{Q}_{n-2} = 1 ,$$

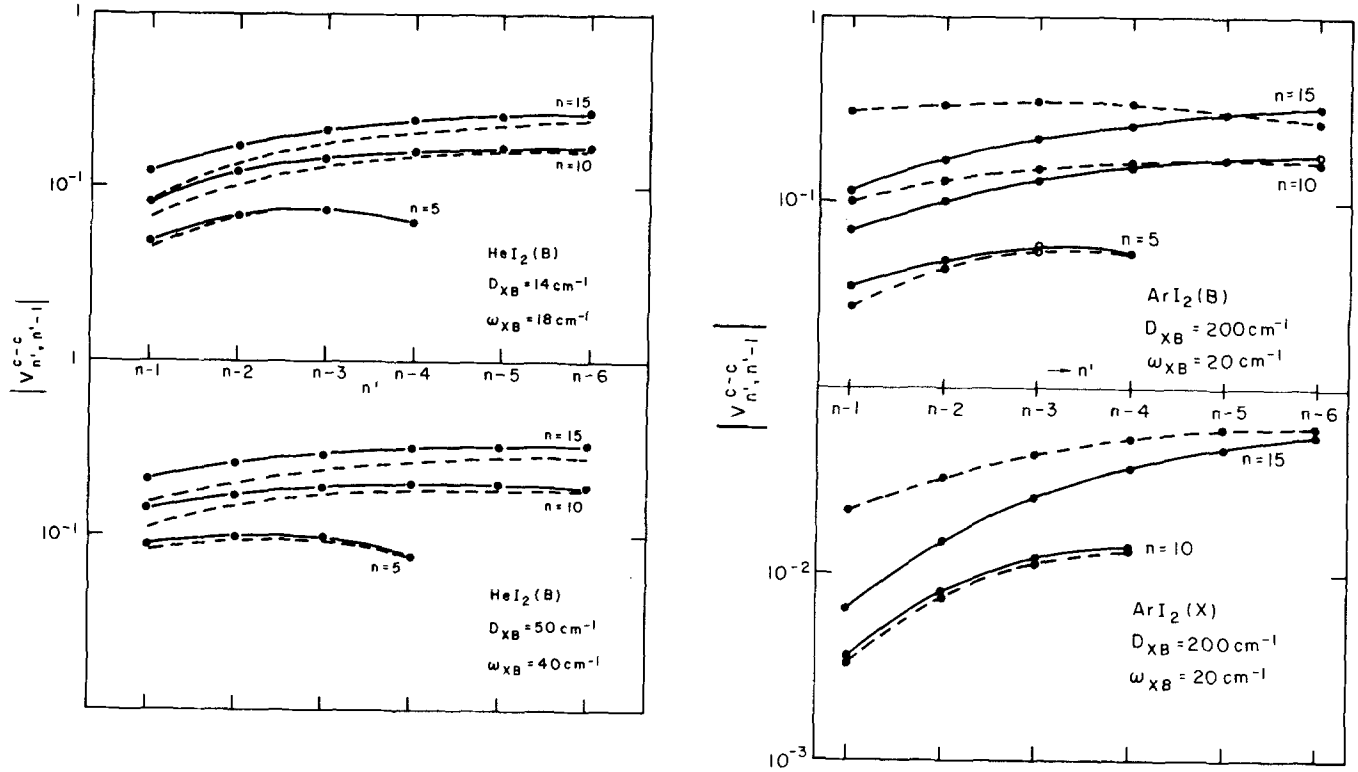

FIG. 4. (a) Effect on the anharmonicity on the continuum–continuum couplings for the VP of $HeI_2(B)$. Solid lines represents on-the-energy-shell continuum–continuum couplings between adjacent continua $|V^{c-c}_{n',n'-1}|$ for an I–I bond represented by an anharmonic potential, while dashed lines correspond to the harmonic approximation. The energy shell is specified by a discrete level (n,l) with n given on the figure and $l=0$. The parameters for the van der Waals interaction are marked on the figure, while the I–I bond parameters were taken from Ref. 17. (b) Same as Fig. 4(a) for VP of ArI_2 linear van der Waals molecule in electronic states $B\,^3\Pi$ and $X\,^1\Sigma$.

$$\bar{Q}_{j-1}=\bar{Q}_j+\pi^2 V_{j,j+1}{}^2\bar{Q}_{j+1}\,, \tag{29b}$$

where n is the vibrational quantum number of the BC bond in the initial discrete state $|nl\rangle$. Equations (23)–(29), together with the explicit expressions for the coupling matrix elements presented in Sec. II, provide a theory of VP on a single electronic potential surface. It is gratifying that for a simple case of a linear VDWM we were able to present the theory of VP in terms of closed analytical expressions. Our treatment incorporates both the effects of discrete–continuum coupling as well as the effects of continuum–continuum coupling. The present description of the VP process involves basically feeding of the continuum states, induced by d–c coupling and a "half-collision" process within the dissociative states on the single potential surface which originates from c–c coupling. A simple-minded approach which disregards the effects of intercontinuum coupling will result in a conventional description of a metastable resonance $|nl\rangle$ decaying into a manifold of uncoupled continua. Under these circumstances $F(n', n'')=\delta_{n',n''}$ and the resonance half-width [Eq. (24)] reduces to the familiar Golden rule result

$$\Gamma^0_{nl}=\pi\sum_{n'}|V^{d-c}_{n',nl}|^2\,, \tag{30}$$

while the vibrational distribution assumes the simple form appropriate for the branching ratio for the decay of a discrete state into a manifold of uncoupled continua[12]

$$P^0_{n'}=|V^{d-c}_{n'nl}|^2\Big/\sum_{n''}|V^{d-c}_{n'',nl}|^2\,. \tag{31}$$

The approximate relations (30) and (31) provide a zero-order description of the VP process and will be useful to explore some of the gross features of this problem.

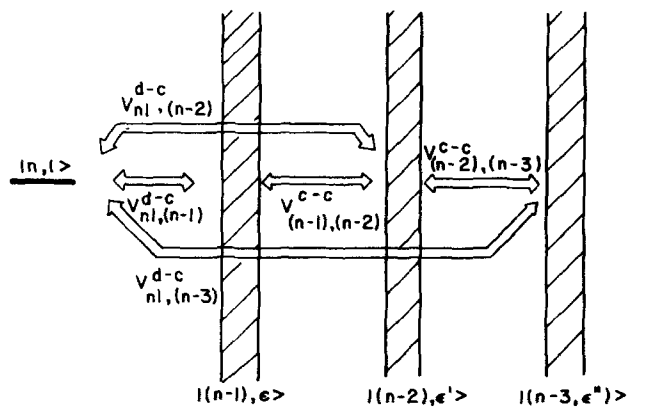

FIG. 5. Simplified level scheme used for the description of vibrational predissociation of a van der Waals molecule X···BC, where X is a rare-gas atom and BC a conventional diatomic molecule. The initially prepared discrete level is denoted by $|n,l\rangle$, where n is the quantum number describing the vibration of BC and l is the quantum number associated with the bound motion of X with respect to BC. This level decays into continuum states $|n',\epsilon\rangle$, where ϵ is the relative kinetic energy for the unbound motion of X with respect to BC and $n'<n$.

It should be mentioned that Rosen's pioneering study[5] of the VP problem just considered this zero-order description. In Sec. IV we shall refrain from numerical calculations and utilize the simple zero-order description to derive some heuristic approximate relations which will be useful for the elucidation of the nature of such processes. As we shall demonstrate in Sec. V the intercontinuum coupling effects will modify both the magnitude of the resonances widths as well as the final vibrational distribution. Thus, any quantitative treatment of the VP problem has to incorporate these contributions.

IV. SOME APPROXIMATE RELATIONS AND CORRELATIONS

In order to explore the gross features of the VP process we shall handle first a grossly oversimplified model when the intermolecular BC bond potential was taken to the harmonic and continuum–continuum coupling effects were neglected. We shall thus consider for the moment the decay width Γ^0_{nl}, given by Eq. (30), which (see Appendix A) can be recast in the form

$$\Gamma^0_{nl} = (\pi/8)\hbar\omega_{BC} n[(2K_{XB} - 2l - 1)/l!\,\Gamma(2K_{XB} - l)]m \times\{\sinh(2\pi y)/[\cos^2\pi K_{XB} + \sinh^2(\pi y)]\}\,|\Gamma(K_{XB} + 1/2 - iy)|^2 , \quad (32)$$

where

$$m = \frac{m_X m_C}{m_B(m_X + m_C + m_B)} , \quad (33a)$$

$$y = [\beta - (K_{XB} - l - 1/2)^2]^{1/2} , \quad (33b)$$

$$\beta = 4D_{XB}\omega_{BC}/\hbar\omega^2_{XB} = 2\omega_{BC}\mu_{X,BC}/\hbar\alpha^2_{XB} . \quad (33c)$$

The total number of levels of the anharmonic oscillator which corresponds to the van der Waals bond is (see Table I)

$$N \sim K_{XB} + 1/2 . \quad (34)$$

We shall be interested in the situation $y \gg 1$, and as for VDWM we expect that $\beta \gg 1$ [as is evident from the condition $\omega_{BC}/\omega_{XB} \gg 1$ in Eq. (33c)]; this state of affairs will prevail for values of l such that $l > \beta^{1/2}$. Equation (32) now simplifies to

$$\Gamma^0_{nl} \sim (\pi/2)\hbar\omega_{BC} n[(N - l - 1)/l'(2N - l - 1)!\,]m\,|\Gamma(N - iy)|^2 . \quad (35)$$

Utilizing the expansion of the Gamma function[16]

$$|\Gamma(N - iy)|^2 = \left\{\prod_{\phi=0}^{N-1}[(N-\phi)^2 + y^2]\right\} 2\pi y \exp(-\pi y) , \quad (36)$$

then for $y \gg N$, Eqs. (35) and (36) result in

$$\Gamma^0_{nl} \simeq \pi^2\hbar\omega_{BC} n[(N - l - 1)/l!\,(2N - l - 1)!\,]m\,y^{2N-1}\exp(-\pi y) , \quad (37)$$

where y is defined in terms of Eqs. (33b) and (33c). When $y \gg N$ and $\beta \gg N$ we can write

$$y \cong \beta^{1/2}[1 - (2\beta)^{-1}(N - l - 1)^2] . \quad (38)$$

Equations (37), (38), and (33c) provide a useful semiquantitative description of the dependence of the VP dynamics on the molecular parameters of the VDWM, such as the molecular frequency ω_{BC}, the dissociation energy of the VDWM D_{XB}, and other parameters of this bond, such as $\mu_{X,BC}$, α_{XB}, or ω_{XB}, all of which are incorporated in the reduced energy parameter β [Eq. (33c)]. This result also accounts for the dependence of the VP rate on the quantum number n of the molecular bond as well as on the quantum number l of the van der Waals bond, at least for high values of the latter. The following comments are now in order.

A. Energy gap law

For a large value of l in the range $l \lesssim N - 1$ we can take $y \simeq \beta^{1/2}$ on Eq. (37), which assumes the form

$$\Gamma^0_{nl} \propto \exp[-\pi\beta^{1/2} + (N - 1/2)\ln\beta] . \quad (39)$$

Utilizing Eq. (33c) the VP half-width is essentially

$$\Gamma^0_n \propto \exp[-2\pi\hbar^{-1/2}(D^{1/2}_{XB}/\omega_{XB})\omega^{1/2}_{BC}] . \quad (40)$$

For a VDWM we expect that $\omega_{BC} \gg D_{XB} > \omega_{XB}$, e.g., $\beta \gg 1$. Thus, the VP rate is expected to decrease fast with increasing of the molecular frequency ω_{BC}, the functional dependence being approximately $\Gamma^0_{nl} \propto \exp(-a\omega^{1/2}_{BC})$. Equation (40) clearly demonstrates that the VP rate will be enhanced by a close matching of the (high) molecular frequency ω_{BC}, which breaks the molecular complex, and the effective stretching frequency ω_{XB} of the van der Waals bond. This central result establishes an energy gap law for VP.

B. Energetic parameters of the VDWM

The VP rate is essentially determined by the reduced energy parameter $2\hbar^{-1/2}(D^{1/2}_{XB}\omega_{XB})\omega^{1/2}_{BC}$. Thus, we expect that $\Gamma^0_{nl} \propto \exp(-bD^{1/2}_{XB}\omega_{XB})$, where b is constant for fixed energetic parameters of the molecular bond BC.

C. Mass effect

To explore the dependence of the VP rate on the mass m_X of the rare-gas atom we consider again Eq. (40) with the alternative definition $\beta = 2\hbar^{-1/2}\omega_{BC}\mu_{X,BC}/\alpha^2_{XB}$ [Eq. (33c)] so that

$$\Gamma^0_{nl} \propto \exp[-2^{1/2}\hbar^{-1/2}\pi(\omega^{1/2}_{BC}/\alpha_{XB})\mu^{1/2}_{X,BC}) . \quad (41)$$

Thus, for a fixed value of the molecular frequency ω_{BC} and provided that the characteristic length α_{XB} depends weakly on the nature of the X atom (see Table I) we expect that (at least for high values of l) $\Gamma^0_{nl} \propto \exp(-c\mu^{1/2}_{X,BC})$, the VP rate being enhanced by decreasing the mass of the rare-gas atom. We note in passing that another contribution to the mass effect originates of course from the adimensional mass m in Eq. (37), so that we should actually write $\Gamma^0_{nl} \propto \mu_{X,BC}\exp(-c\mu^{1/2}_{X,BC})$. However, the effect of the pre-exponential factor is smaller than that of the exponential term.

D. Dependence on the quantum number n

It is evident from Eqs. (32) and (37) that $\Gamma^0_{nl} \propto n$, the VP rate being enhanced with increasing of the vibrational quantum number of the BC bond. This linear dependence of Γ^0_{nl} on n obtained here is common to all problems where the harmonic approximation is invoked. Anharmonicity effects (see Sec. V) will result in a superlinear dependence of Γ^0_{nl} on n.

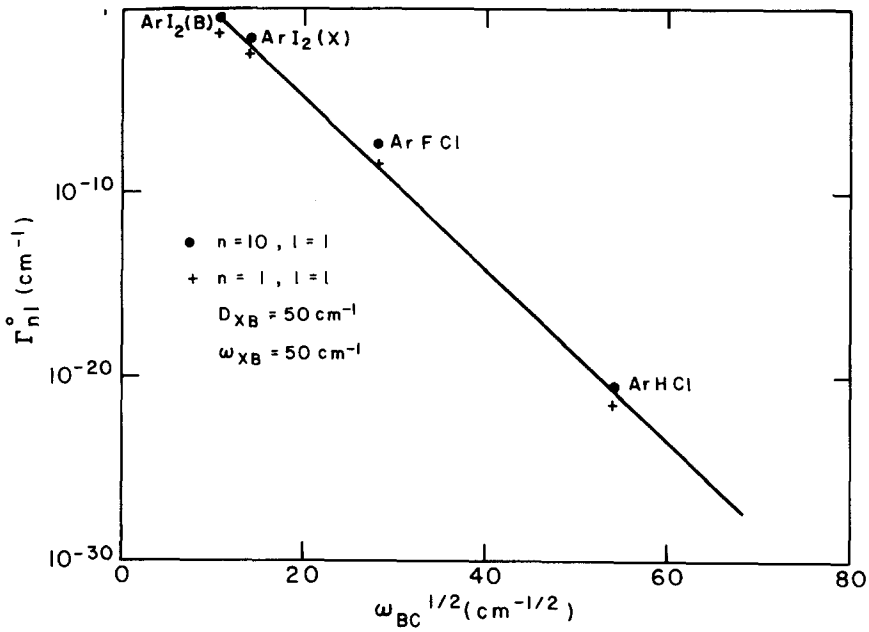

FIG. 6. Dependence of the VP rate on the intramolecular frequency ω_{BC}. The calculations were performed for an harmonic BC potential, neglecting continuum–continuum couplings. The points correspond to the VP from the level $n=10$, $l=1$, while the crosses correspond to $n=1$, $l=1$. The parameters for the van der Waals interaction are marked on the figure.

E. Dependence on the vibrational quantum number l

From Eqs. (37) and (38) it is evident that for high values of $l \lesssim N-1$ the VP rate increases with decreasing l. When the l dependence is explicitly incorporated in Eq. (37) we observe that

$$\Gamma^0_{nl} \propto \exp[(2\pi/\beta^{1/2})(N-l-1)^2] \,. \tag{42}$$

The simple approximate relations obtained herein are extremely useful for the elucidation of the gross features of the VP problem. However, up to this point we were concerned only with the implications of bound–continuum coupling effects. We shall now proceed to the study of the results of the global theory developed in Sec. III which will enable us to incorporate the effects of continuum–continuum coupling.

V. MODEL CALCULATIONS OF VIBRATIONAL PREDISSOCIATION

We have presented in Sec. III explicit, analytical results for the rate and for the vibrational distribution of the products in VP of linear triatomics. In what follows we shall attempt to account for some features of the VP of linear rare-gas–diatomic VDWM's. The basic input data involve the well-known[17] spectroscopic parameters for the molecular BC bond and the potential parameters for the van der Waals bond. For the latter we have utilized the currently available information summarized in Table I. These potential parameters ω_{BC} for the harmonic molecular bond (or ω_{BC} and D_{BC} for the anharmonic BC bond), and α_{XB} and D_{XB} for the van der Waals bond, together with the reduced masses μ_{BC} and $\mu_{X,BC}$, determine both the d–c and the c–c coupling terms. In the absence of detailed experimental results for linear VDWM's we shall utilize the complete theory to derive a set of theoretical predictions.

A. Energy gap law for VP

To explore the gross features of the dependence of the VP rate on the energetic parameters of the VDWM we portray in Fig. 6 a sample of numerical results of model calculations for a number of such molecules. The BC bond was taken to be harmonic and for the sake of a simplified representation of the VP rate over a wide range (20 orders of magnitude) of Γ_{nl} we have disregarded again the effects of c–c coupling. These data for a series of linear VDWM's, where the normal BC bond frequency varies in the range 128–3000 cm^{-1}, exhibit the energy gap law for VP, the rate decreasing with increasing $\omega_{BC}^{1/2}$ in accord with the prediction of Eq. (40). We note in passing that in view of some changes in the mass parameters appropriate for different molecules there are some changes in the exponential parameter a, in the relation $\Gamma^0_{nl} \propto \exp(-a\omega_{BC}^{1/2})$; however, these are overwhelmed by the changes in the molecular frequency, which leads to a variation of Γ^0_{nl} over 20 orders of magnitude for a series of related linear VDWM's.

B. Anharmonicity effects

To provide a visual demonstration of the dependence of the VP rate on the vibrational quantum number n of the BC bond we present in Figs. 7(a)–7(c) the results of model calculations of Γ^0_{nl} for $l=\bar{l}$, where the VP rate reaches its maximum value for a given n. In these calculations c–c coupling effects were again disregarded. For the harmonic BC potential [Eq. (2a)] Γ^0_{nl} exhibits a linear dependence on n, $\Gamma^0_{nl} = A \cdot n$, where A is a constant in accord with Eqs. (32) and (37). When an anharmonic bond potential [Eq. (2b)] is utilized the increase of the VP rate with n is superlinear and can be fit by the relation $\Gamma^0_{nl} \simeq A \cdot n + B \cdot n^2$, where A and B are constants for a given VDWM. As is evident from Figs. 7(a)–7(c) anharmonicity effects have a minor influence on the VP rate for low values of n, as expected; however, for high n values the anharmonicity of the BC bond considerably enhances the VP rate. This result can be easily rationalized by noting that anharmonicity decreases the effective energy gap between the levels nl and $(n-1)l$, resulting in a somewhat better matching

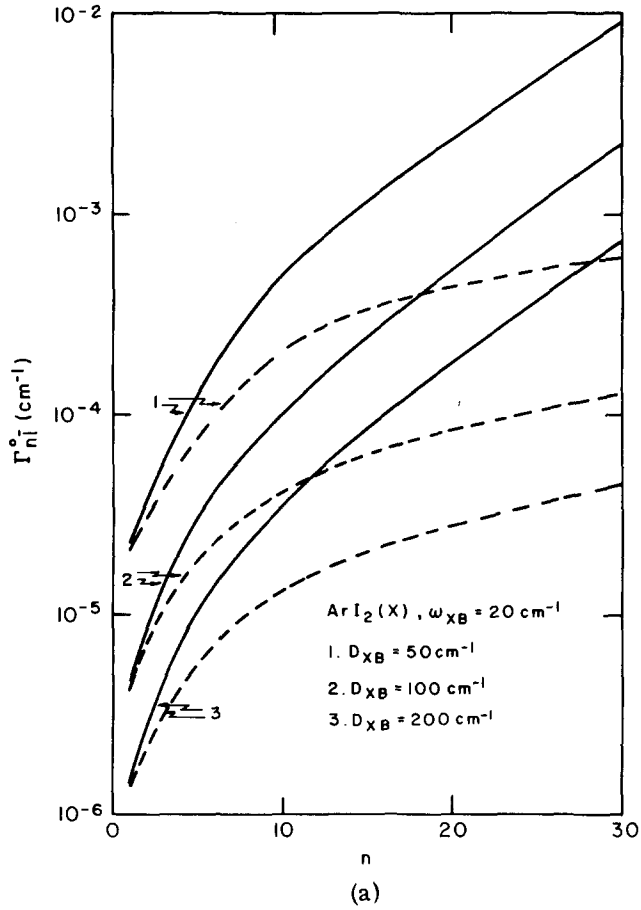

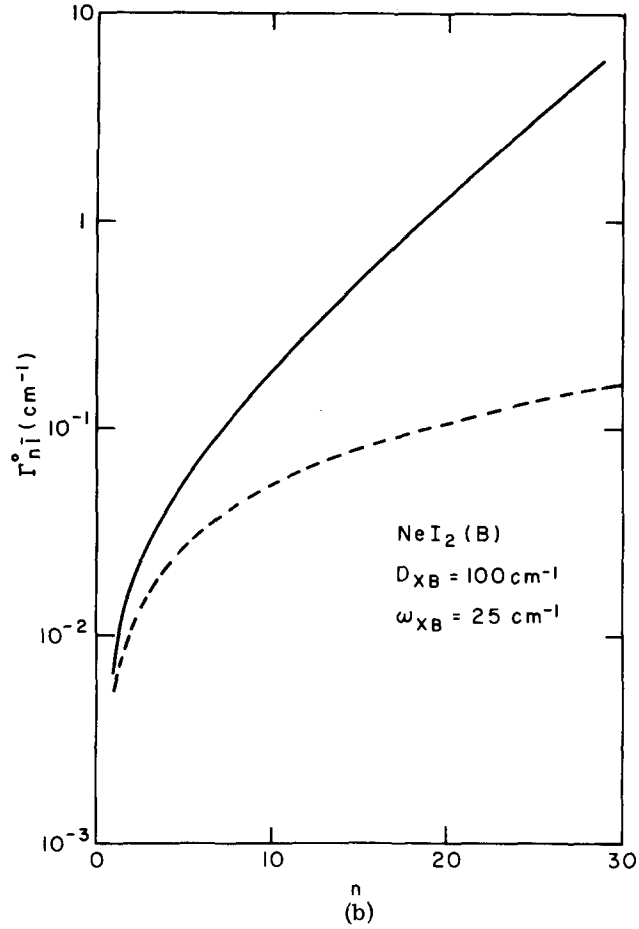

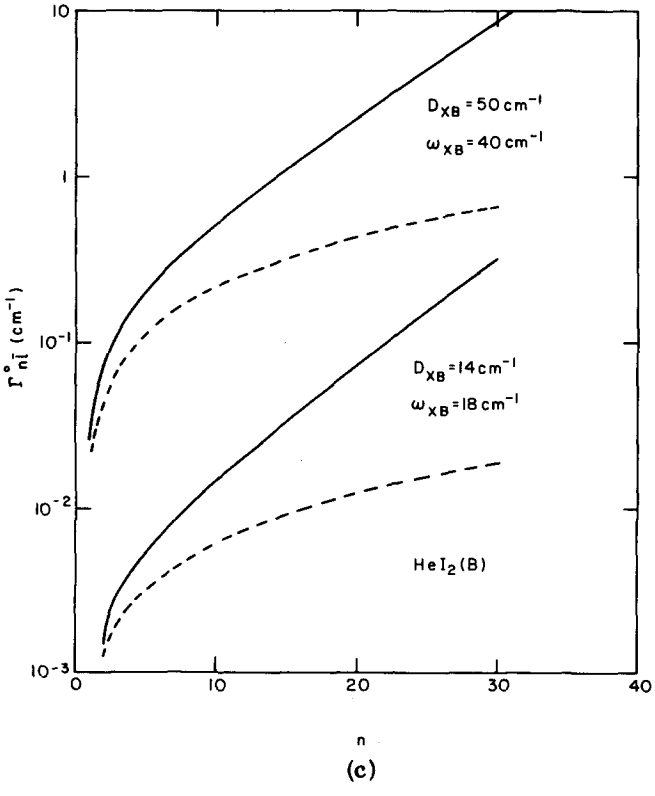

FIG. 7. (a) Model calculations of the dependence of the VP rate for a linear $ArI_2(X)$ van der Waals molecule, neglecting intercontinuum couplings, on the vibrational quantum number n of the $I_2(X)$ bond. Dashed lines represent the values of $\Gamma^{0}_{n\bar{l}}$ calculated in the harmonic approximation for the I_2 molecule, while solid lines correspond to an anharmonic I–I bond characterized by a Morse potential. The parameters of the van der Waals interaction are marked on the figure, while those of the $I_2(X)$ bond were taken from Ref. 17. (b) Same as Fig. 7(a) for linear $NeI_2(B)$. (c) Same as Fig. 7(a) for linear $HeI_2(B)$.

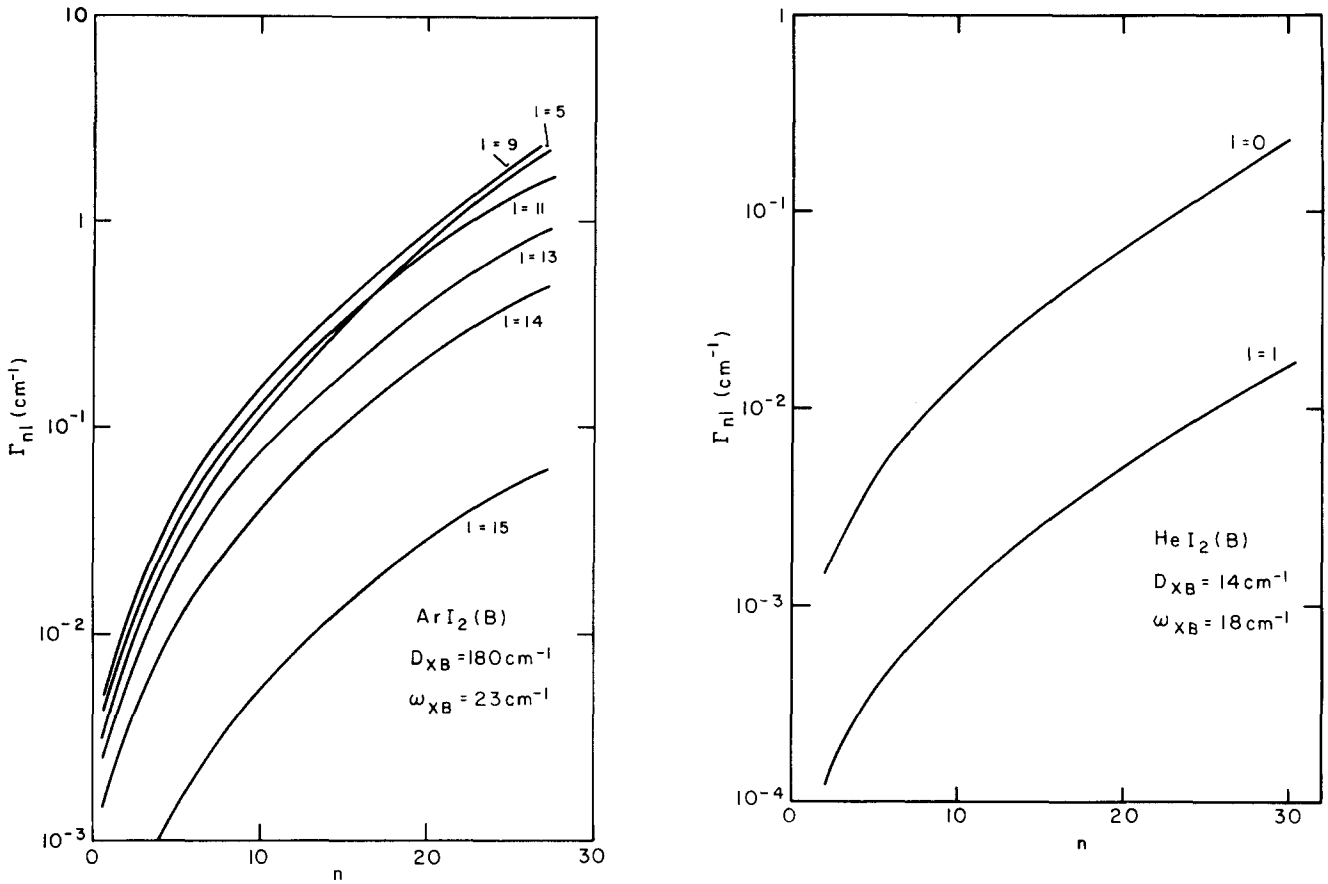

FIG. 8. (a) Model calculations of the dependence of the VP rate from an initial discrete level (n,l) of a linear $ArI_2(B)$ van der Waals on the vibrational quantum number n for different values of l. The I–I bond is anharmonic and has been characterized by a Morse potential with parameters taken from Ref. 17. The parameters of the van der Waals interaction are marked on the figure. The rate Γ_{nl} in cm^{-1} include continuum–continuum interaction. (b) Same as Fig. 8(a) for linear $HeI_2(B)$.

between the vibrational energy of the BC bond which is transferred to the van der Waals bond and the dissociation energy of the latter, thus resulting in a considerable enhancement of the VP rate at high values of n.

C. Dependence of VP rate on l

To assess the dependence of the VP rate on the vibrational quantum number l of the bound states of the van der Waals bond we have conducted a series of calculations of Γ_{nl} which incorporates both the effects of d–c and of c–c coupling. These results are summarized in Figs. 8–10. From Figs. 8(a) and 8(b) it is apparent that for a VDWM where the weak bond supports a small number of bound states the VP rate at constant value of n increases with decreasing l [see also Fig. 9(a)], while when the number of bound states is large Γ_{nl} increases with decreasing l for high values of l, reaching a maximum at some value $l=\bar{l}$ and then subsequently decreases with further decrease of l [see Figs. 8(b) and 9(b)]. The increase of Γ_{nl} with decreasing l at high values of l is in accord with the simple analysis of Sec. IV.C. From Fig. 9(b) we can assert that for a given VDWM the value of $\bar{l}$ is practically invariant to changes in the molecular bond quantum number n. Finally, from Fig. 10 we note that anharmonicity effects just scale all the values of Γ_{nl} for a given value of n and do not modify the gross features of the dependence of the VP rate on l.

D. Effects of continuum-continuum coupling

The incorporation of continuum–continuum coupling effects in the general formalism of the VP problem advanced in Sec. III enabled us to go beyond the simple Golden rule type calculation and to incorporate the features of the half-collision problem on a single potential surface in a self-consistent manner. We have conducted a series of model calculations of the VP rate using the general model which incorporates the effects of both d–c and c–c coupling and compared the data with the results of calculations using the simple Golden rule expression (30). The data were calculated for the anharmonic BC bond for $l=\bar{l}$. As is evident from Figs. 11(a)–11(c) the effects of intercontinuum couplings are rather small for low values of n. However, at higher values of n the VP rate is retarded by intercontinuum coupling effects and $\Gamma_{nl} \sim (0.3-0.5)\Gamma^0_{nl}$. Such a retardation effect due to coupling between "smooth" continua, where the c–c interaction is weakly varying with energy, is well known in the theory of relaxation phenomena.[18]

E. Final vibrational distribution

Another interesting physical consequence of the continuum–continuum coupling involves the final vibrational distribution of the diatomic product in the VP process $XBC(nl) \rightarrow X + BC(n')$. When intercontinuum

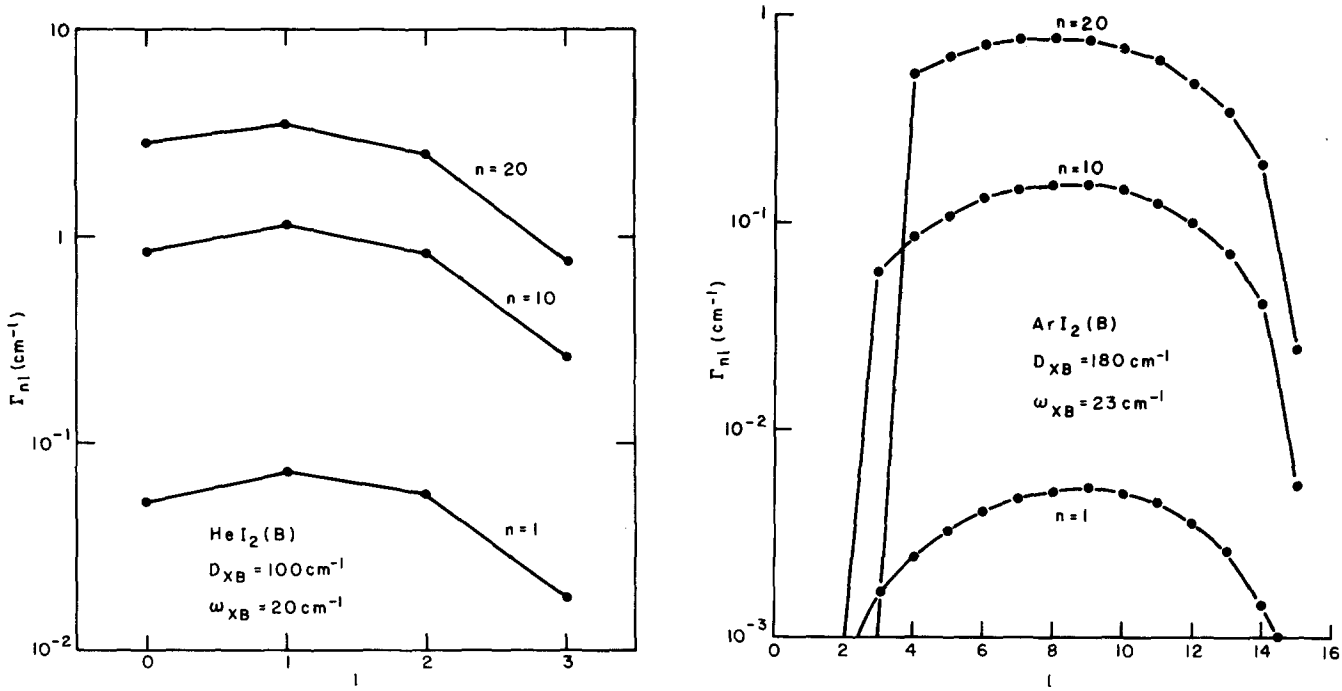

FIG. 9. (a) Model calculations of the dependence of the VP rate from an initial discrete level (n,l) of a linear $HeI_2(B)$ van der Waals molecule on the quantum number l for different values of n. The I-I bond is anharmonic and has been characterized by a Morse potential with parameters taken from Ref. 17. The parameters of the van der Waals bond are marked on the figure. The rate Γ_{nl} in cm^{-1} include continuum–continuum interaction. (b) Same as Fig. 7(a) for linear $ArI_2(B)$.

coupling effects are disregarded Eq. (31) clearly demonstrates that the branching ratio for the population of different vibrational states $n'(<n)$ of the diatomic fragment is determined by the squares of the d–c coupling terms. Following the technical discussion of Sec. II we recall that the $V^{d-c}_{nl,n',\epsilon}(n'<n)$ terms evaluated on the energy shell are dominated by the term $n'=n-1$ and are negligibly small for $n'<(n-1)$ (see Fig. 2). Without alluding to any further numerical calculations we can assert that provided c–c coupling effects are disregarded the dominating decay channel of the $|nl\rangle$ initial state will involve the population of the $(n-1)$ state of the fragment. Intercontinuum coupling effects may result in relaxation of the propensity rule $\Delta n=1$. As is evident from Figs. 12(a)–12(c) we note that $P_{n-1}\simeq 0.6$–0.7 and lower vibrational states may be populated for $ArI_2(B)$, but $P_{n-1}\simeq 0.9$–1 for $HeI_2(B)$.

F. Dependence of VP rate on parameters of the VDWM

The model calculations of the VP rate Γ_{nl} displayed in Figs. 11(a)–11(c) exhibit all the general features which emerge from the semiquantitative analysis of Sec. IV. In particular, we note that for a given VDWM (ω_{BC} fixed) $\ln(\Gamma_{nl})$ is essentially determined by $D_{XB}^{1/2}\omega_{XB}^{-1}$, so that Γ_{nl} decreases with increasing D_{XB} at constant ω_{XB} and Γ_{nl} increases with increasing ω_{XB} at constant D_{XB}, in accord with Eq. (40). As the effective frequency ω_{XB} is not the experimental observable frequency, it may be more useful perhaps to relate the VP rate to the inverse length α_{XB} of the Morse potential where according to Eq. (41) for a given VDWM (ω_{BC} and $\mu_{X,BC}$ fixed) $\ln(\Gamma_{nl})\propto\alpha_{XB}^{-1}$. This expectation is borne out by the numerical results of Fig. 11(a). Next, it is of interest to consider the mass effect on VP and to

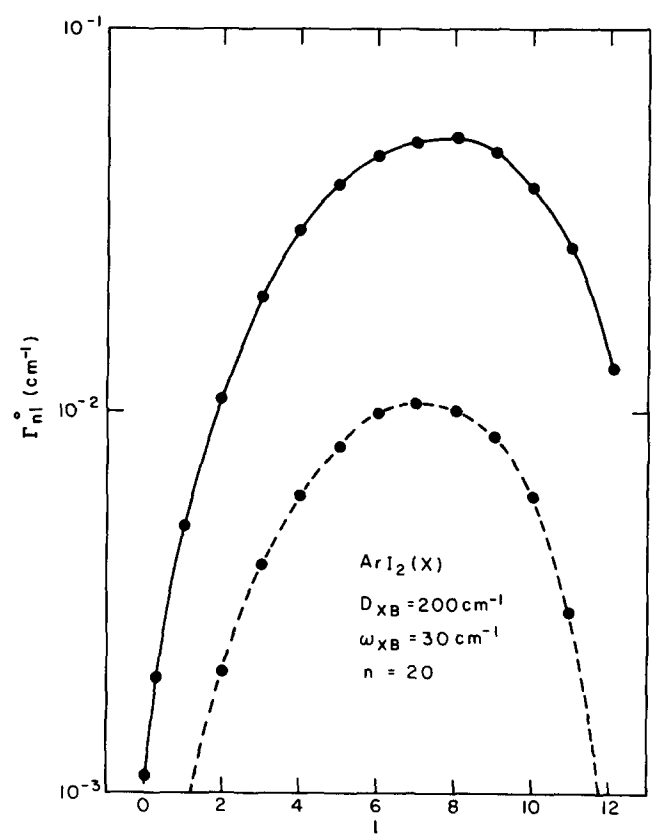

FIG. 10. Model calculations for the VP rate of linear $ArI_2(X)$ neglecting continuum–continuum interaction in the function of the quantum number l of the initial discrete level $|n,l\rangle$, where $n=20$. Dashed lines represent the results for an harmonic I–I bond, while the solid line connects the points obtained for an anharmonic I–I bond characterized by a Morse curve with parameters taken from Ref. 17. The parameters of the van der Waals interaction are marked on the figure.

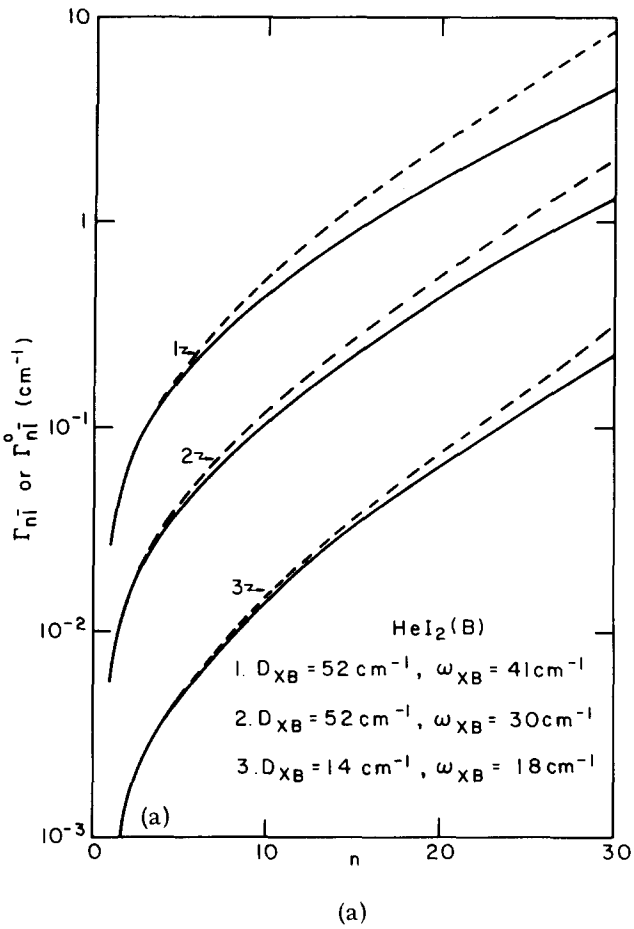

(a)

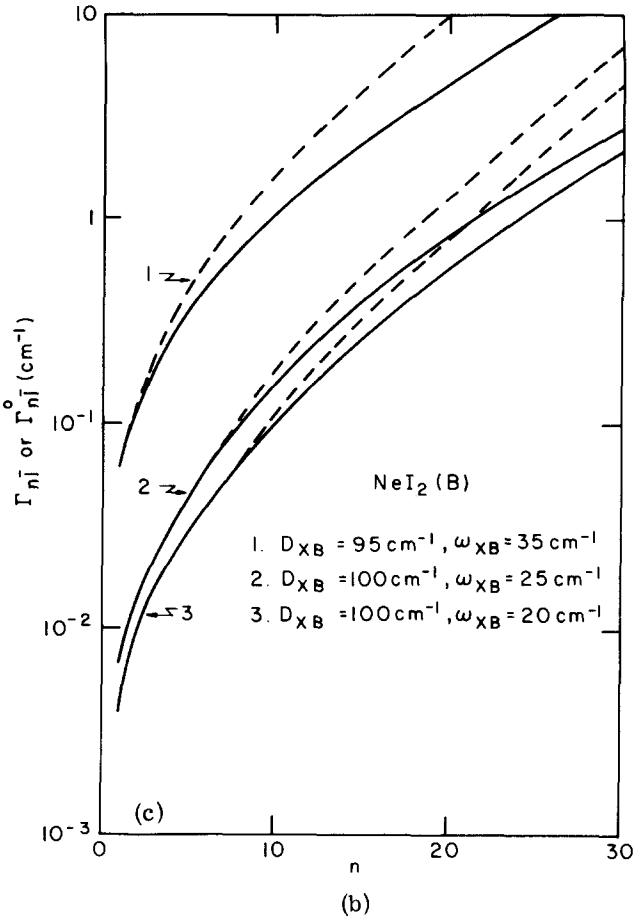

(b)

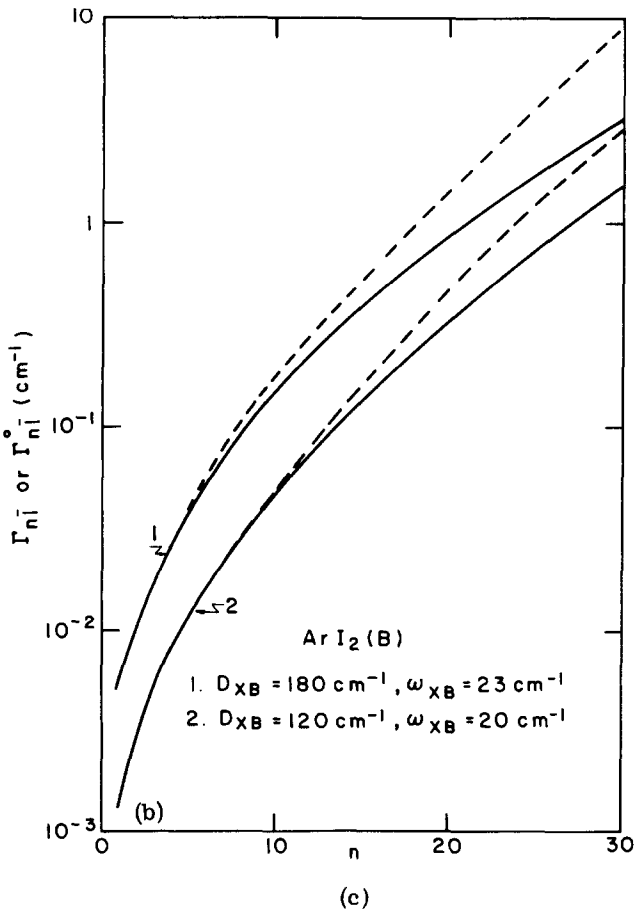

(c)

FIG. 11. (a) Model calculations for the VP rate of linear $HeI_2(B)$ in function of the vibrational quantum number n of the initial discrete level $|n,\bar{l}\rangle$. Dashed lines are the results obtained by neglecting continuum–continuum interaction (Γ^0_{nl}), while solid lines correspond to the results for $\Gamma_{n\bar{l}}$. The I–I bond is characterized by a Morse potential with parameters taken from Ref. 17. The parameters of the van der Waals interaction are marked on the figure. (b) Same as Fig. 11(a) for $NeI_2(B)$. (c) Same as Fig. 11(a) for $ArI_2(B)$.

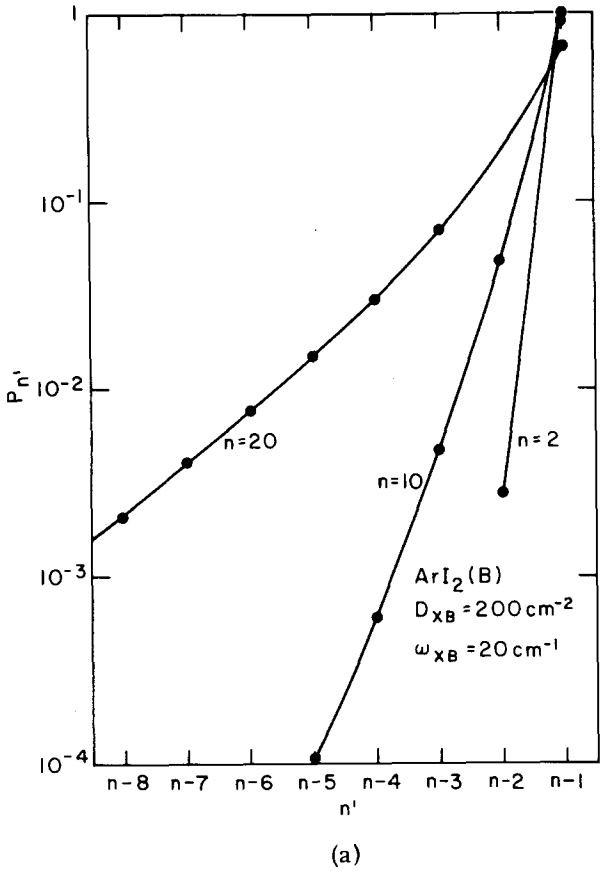

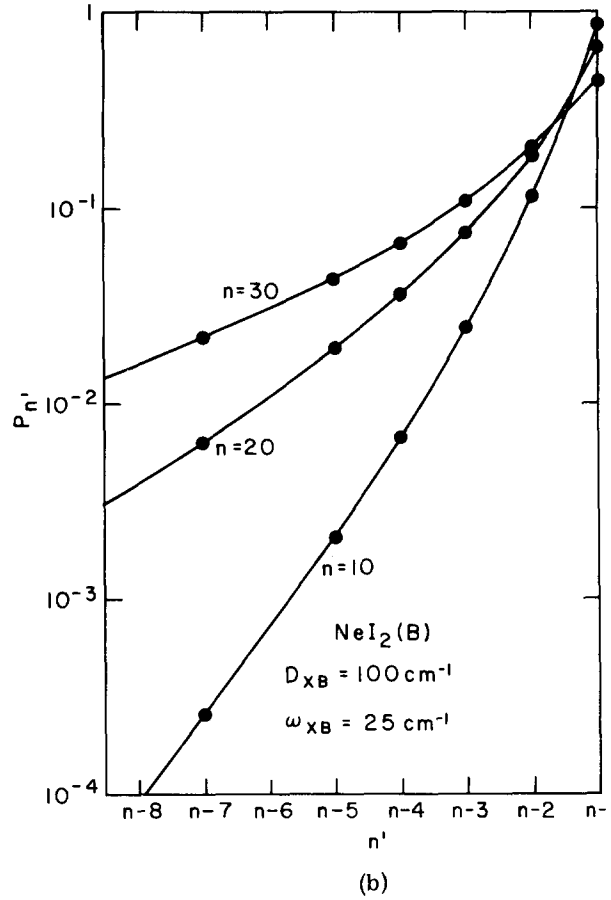

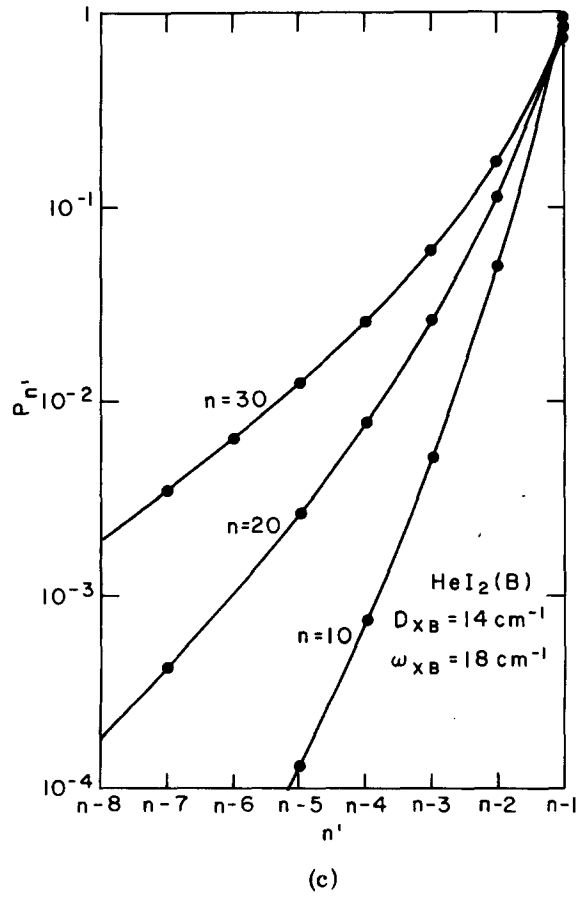

FIG. 12. (a) Vibrational distribution of the I_2 molecule resulting from an initial state of $ArI_2(B)$ characterized by quantum number n and $\bar{l}$, The I_2 bond is described by a Morse potential with parameters taken from Ref. 17. The parameters of the van der Waals interaction are marked on the figure. (b) Same as Fig. 12 for $NeI_2(B)$. (c) Same as Fig. 12(a) for $HeI_2(B)$.

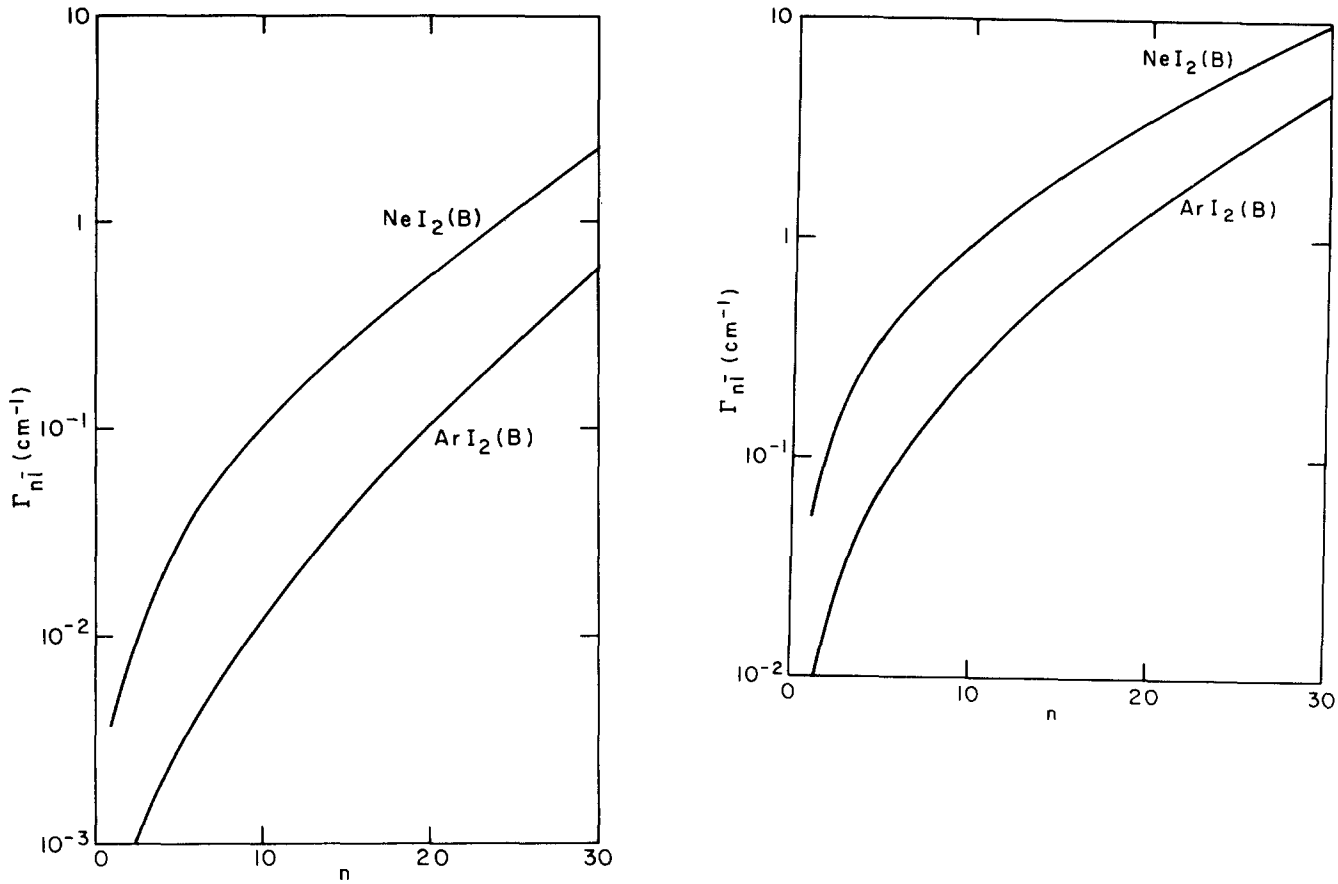

FIG. 13. (a) Model calculations of the mass effect on the VP rate of linear X$\cdots$$I_2(B)$, (X≡Ne, Ar) molecules. The I_2 molecule is characterized by a Morse potential with parameters taken from Ref. 17. The potential parameters for the van der Waals bond are fixed for the two molecules and are equal to $D_{XB}=200$ cm^{-1}, $\alpha_{XB}=1.245$ Å^{-1}. (b) Same as Fig. 13(a) with $D_{XB}=100$ cm^{-1}, $\alpha_{XB}=1.245$ Å^{-1}.

investigate the dependence of $\Gamma_{n\bar{l}}$ on the mass m_X of the rare-gas atom. In Figs. 13(a) and (13b) we desplay some results of model calculations of $\Gamma_{n\bar{l}}$ for a series of X–$I_2(B)$ (X=Ne, Ar) linear molecules. It is evident that for a fixed value of the Morse potential parameter α_{XB}, $\Gamma_{n\bar{l}}$ increases with decreasing of the mass of the rare-gas atom. This result concurs with the prediction of Eq. (41).

VI. CONCLUDING REMARKS

We were able to advance a physical model which incorporates all the physical features of VP of linear triatomic VDWM's. The results of the present study can be confronted with experiment and will be hopefully of use for establishing general relations and correlations of experimental data, once these become available. At the present stage several experimental implications of the present study should be considered.

(1) The energy gap law for VP of VDWM's has some general implications. First, VDWM's characterized by a high molecular frequency ω_{BC} are expected to be stable with respect to VP processes on the time scale of the radiative decay of the vibrationally excited or electronic–vibrational excited states. Typical rates for ir decay in the ground electronic state are $\delta_{ir}\sim 10^{-8}$ cm^{-1}, while the decay rate from electronic–vibrational excited states is $\delta_e\sim 10^{-3}$–10^{-5} cm^{-1}. When $\gamma_{nl}\ll\delta_{ir}$ no VP in the ground electronic surface will occur, and when $\gamma_{nl}\ll\delta_e$ the electronic excited states of the VDWM will be stable with respect to VP. The stabilities of the vibrationally excited Cl_2–Cl_2^* VDWM with respect to VP[19] on the ground electronic potential surface reflects an interesting implication of the energy gap law. This complex is characterized by a high frequency of the intramolecular Cl–Cl bond ($\omega_{BC}\simeq 565$ cm^{-1}), making the exchange of vibrational energy between the molecular bond and the weak van der Waals bond ineffective on the time scale of the lifetime of the vibrationally excited state. Second, as the intramolecular frequency ω_{BC} is in general lower in the electronic excited configuration, we expect that the VP process in an electronically excited state will be faster than in the ground electronic state, provided the energetic parameters of the van der Waals bond are not substantially modified. We note in passing that the X–I_2 (X≡He, Ne, Ar) molecules studied by Kim, Smalley, Wharton, and Levy[4] provide ideal candidates for probing the dynamics of VP processes in view of the low frequency of I_2 bond in the ground ($X^1\Sigma$) and in the electronically excited ($B^3\Pi$) configurations. The VP rates of these XI_2 molecules are expected, of course, to be higher in the electronically excited state as in the ground state.

(2) The increase of the VP rate for HeI_2 in the $B^3\Pi$

state of I_2 with n is found to be superlinear with increasing of the vibrational quantum number n of the I–I bond.[4(a),4(b)] This experimental result concurs with our conclusions (see Sec. V. B) concerning anharmonicity effects on VP.

(3) Regarding theoretical predictions of the absolute values of VP rates which emerge from the present model these should be viewed with considerable caution. Obviously, the quantitative treatment is inapplicable for the T-shaped HeI_2 molecule. For the linear $ArI_2(B)$ complex we predict, using the potential parameters $D_{XB}=100-200$ cm^{-1}, $\alpha_{XB}=1.25$ Å^{-1}, that for $n=1$ the total VP rate is $\sim 3\times10^{9}-2\times10^{8}$ sec^{-1}, and for $n=10$ it is $\sim 1\times10^{11}-5\times10^{9}$ sec^{-1}, while being for $n=20$ $5\times10^{11}-4\times10^{10}$ sec^{-1} [note that the total VP rate is equal to $2\Gamma_{nl}/\hbar$, Eq. (23)]. The spread of the rates for each value of n reflects the result for the range of the potential parameters specified above. Experimental results for the ArI_2 system are not yet available. We note in passing that these rough estimates of the VP rates for the linear ArI_2 are of the same order of magnitude as experimentally observed[4(a),4(b)] for the T-shaped $HeI_2(B)$ complex.

(4) Concerning the final vibrational distribution of the products Kim *et al.*[4(b)] have recently reported that the propensity rule $\Delta n=1$ holds extremely well for VP of the T-shaped HeI_2(B) and $P_{n-1}>0.98$, if the initial discrete state has vibrational quantum number n for the BC bond. Our calculations (Sec. V. E) indicate that for a linear VDWM, such as $ArI_2(B)$, P_{n-1} provides the dominant contribution to the vibrational distribution of the fragments $P_{n-1}=0.6-0.7$, but the lower vibrational states $n'<n-1$ are also populated. On the other hand, for a linear $HeI_2(B)$ molecule our results show, indeed, a very good agreement with the propensity rule. It will be quite superficial to confront this theoretical prediction for the linear VDWM with the available results for the T-shaped molecule, and further experimental information is obviously required for the dynamics of a linear complex.

We have repeatedly emphasized that the results of the present theoretical treatment of VP are inapplicable for the T-shaped $HeI_2(B)$ complex for which the most extensive experimental data are currently available. We have performed a theoretical investigation of the VP dynamics of a T-shaped VDWM, considering a perpendicular VP process.[20] This perpendicular problem does not result in an analytical solution, in contrast to the linear case, and numerical methods had to be applied. A by-product of this analysis involved the application of the same numerical brute force methods to the linear VP problem. The results of that numerical experiment for the linear case were found to reproduce the analytical results of the present work, which rest upon the formalism of Sec. III, with good accuracy, thus providing a nice confirmation of the numerical data presented herein. A report on that work will be presented elsewhere.[20]

After this paper was submitted for publication we have become aware of several recent theoretical contributions to the interesting field of VP of VDWM's. Ashton and Child[21(a),(b)] have utilized a semiclassical dumbbell model to study the VP of ArHCl. They find that the VP rate is surprisingly slow, which is in accord with our general conclusions and which rest on the energy gap law. Ewing[21(c)] has addressed himself to the role of VP in vibrational relaxation and derived an approximate expression for the VP rate.

ACKNOWLEDGMENTS

We are indebted to Professor D. H. Levy for prepublication information. This research was completed when one of us (J. Jortner) was a Sherman Fairchild Distinguished Scholar at the California Institute of Technology, Pasadena, CA. J. J. is indebted to the Division of Chemistry and Chemical Engineering at the California Institute of Technology for their hospitality.

APPENDIX A: ANALYTIC EVALUATION OF THE COUPLING MATRIX ELEMENTS

The matrix elements of the residual potential (7b) can be written, in general, as

$$V^{a-b}_{n\alpha,n'\beta}=(A^{(2)}_{nn'}B^{(2)}_{\alpha\beta}-2A^{(1)}_{nn'}B^{(1)}_{\alpha\beta}), \tag{A1}$$

where a, $b\equiv d$ or c (discrete or continuum); α, $\beta\equiv l$ or ϵ;

$$B^{(j)}_{\alpha\beta}=D_{XB}\int dR_{X,BC}\,\phi_\alpha(R_{X,BC}) \times e^{-j\alpha_{XB}(R_{X,BC}-\bar{R}_{X,BC})}\phi_\beta(R_{X,BC}), \quad j=1,2; \tag{A2}$$

and $A^{(j)}_{nn'}$, $j=1$, 2 are given in Eqs. (12), (14a), and (14b). In order to perform the integration in Eq. (A2) it is necessary to find the discrete and continuum eigenfunctions $\phi_\alpha(R_{X,BC})$ of the $H_{X,BC}$ Hamiltonian defined in Eq. (7a). The discrete normalized eigenfunctions are given by[5]

$$\phi_l(R_{X,BC})=\left[\frac{(2K_{XB}-2l-1)\alpha_{XB}}{l!\,\Gamma(2K_{XB}-l)}\right]^{1/2}Z^{-1/2}W_{K_{XB},K_{XB}-l-1/2}(Z), \tag{A3}$$

where

$$Z=2K_{XB}\,e^{-\alpha_{XB}(R_{X,BC}-\bar{R}_{X,BC})} \tag{A4}$$

with $W_{\kappa,\mu}(Z)$ being the Whittaker's function.[16] The dimensionless parameter K_{XB} is defined in Eq. (13c). The eigenvalues associated with the functions (A3) are

$$W_l=-(h^2\alpha_{XB}/2\mu_{X,BC})(K_{XB}-l-1/2)^2, \quad l=0,1,\ldots,\ \text{integer}\ (K_{XB}-1/2). \tag{A5}$$

The energy-normalized continuum eigenfunctions are similarly given by[5]

$$\phi_\epsilon(R_{X,BC})=(\pi\hbar)^{-1}[(\mu_{X,BC}/\alpha_{XB})\sinh(2\pi\theta_\epsilon)]^{1/2} \times|\Gamma(1/2-K_{XB}-i\theta_\epsilon)|\,Z^{-1/2}W_{K_{XB},i\theta_\epsilon}(Z), \tag{A6}$$

with θ_ϵ defined in Eq. (13d).

Using the integrals[5]

$$\int_0^\infty W_{K,K-l'-1/2}(Z)W_{K,K-l-1/2}(Z)\,dZ = \Gamma(l'+1)\,\Gamma(2K-l')[l'(2K-l'-1)-l(2K-l-1)+2K] \tag{A7a}$$

and

$$\int_0^\infty W_{K,K-l'-1/2}(Z)W_{K,K-l-1/2}(Z)(dZ/Z)$$
$$= \Gamma(l'+1)\Gamma(2K-l') , \quad \text{(A7b)}$$

valid for $l' > l-1$, we obtain by replacing Eq. (A3) into (A2) and making use of Eq. (A4)

$$B^{\{1\}}_{l',l} = (D_{XB}/2K_{XB})\left[\frac{(2K_{XB}-2l-1)(2K_{XB}-2l'-1)}{l!\,l'!\,\Gamma(2K_{XB}-l)\Gamma(2K_{XB}-l')}\right]^{1/2}$$
$$\times\Gamma(l'+1)\Gamma(2K_{XB}-l') , \quad l' > l-1 , \quad \text{(A8a)}$$

$$B^{\{2\}}_{l',l} = (B^{\{1\}}_{l',l}/2K_{XB})[l'(2K_{XB}-l'-1)$$
$$-l(2K_{XB}-l-1)+2K_{XB}] , \quad l' > l-1 . \quad \text{(A8b)}$$

Equations (A8a) and (A8b), together with Eqs. (A1), (12), (14a), and (14b), give the final analytical expression for the discrete–discrete coupling $V^{d-d}_{nl,n'l'}$.

The continuum–continuum coupling $V^{c-c}_{n\epsilon,n'\epsilon'}$ given in Eqs. (15), (16a), and (16b) are obtained by replacing Eq. (A6) into (A2) and by making use of the integrals[10]

$$\int_0^\infty W_{K,i\theta}(Z)W_{K,i\theta'}(Z)\,dZ = 2\pi^2(\cosh 2\pi\theta - \cosh 2\pi\theta')^{-1}$$
$$\times\left[\frac{\theta'^2-\theta^2+2K}{|\Gamma(1/2-K+i\theta)|^2} + \frac{\theta'^2-\theta^2-2K}{|\Gamma(1/2-K+i\theta')|^2}\right] \quad \text{(A9a)}$$

and

$$\int_0^\infty W_{K,i\theta}(Z)W_{K,i\theta'}(Z)\,(dZ/Z) = 2\pi^2(\cosh 2\pi\theta - \cosh 2\pi\theta')^{-1}$$
$$\times[\,|\Gamma(1/2-K+i\theta)|^{-2} - |\Gamma(1/2-K+i\theta')|^{-2}] . \quad \text{(A9b)}$$

Finally, the discrete–continuum coupling $V^{d-c}_{nl,n'\epsilon}$ are obtained by placing Eqs. (A3) and (A6) into (A2) and by making use of the integrals[5]

$$\int_0^\infty W_{K,i\theta}(Z)W_{K,K-l-1/2}(Z)\,dZ$$
$$= |\Gamma(1/2+K-i\theta)|^2[(K-l-1/2)^2+\theta^2+2K] \quad \text{(A10a)}$$

and

$$\int_0^\infty W_{K,i\theta}(Z)W_{K,K-l-1/2}(Z)(dZ/Z) = |\Gamma(1/2+K-i\theta)|^2 . \quad \text{(A10b)}$$

The final result is given in Eqs. (11), (13a), and (13b), together with Eqs. (14a) and (14b). A simplified expression can be obtained for the harmonic case if the presumably good approximation

$$\exp[j\alpha_{XB}\gamma(R_{BC}-\bar{R}_{BC})] - 1 \cong j\alpha_{XB}\gamma(R_{BC}-\bar{R}_{BC}) \quad \text{(A11)}$$

is used in Eq. (12). Using the well-known result for harmonic oscillators

$$\int_{-\infty}^\infty \chi_n(R_{BC})(R_{BC}-\bar{R}_{BC})\chi_{n'}(R_{BC})\,dR_{BC}$$
$$= (\hbar/2\mu_{BC}\omega_{BC})^{1/2}[n^{1/2}\delta_{n',n-1} + (n+1)^{1/2}\delta_{n',n+1}] \quad \text{(A12)}$$

the approximate result given in Eq. (32) is obtained.

APPENDIX B: RELATIVE COORDINATES TREATMENT OF VIBRATIONAL PREDISSOCIATION

An alternative description of vibrational predissociation for a linear VDWM can be obtained in terms of Rosen's relative coordinates treatment.[5] This amounts to a choice of the two interatomic distances R_{BC} and R_{XB} as independent coordinates. The nuclear Hamiltonian then becomes

$$H = -\frac{\hbar^2}{2\mu_{BC}}\frac{\partial^2}{\partial R^2_{BC}} - \frac{\hbar^2}{2\mu_{XB}}\frac{\partial^2}{\partial R^2_{XB}}$$
$$+\frac{\hbar^2}{m_B}\frac{\partial^2}{\partial R_{BC}\partial R_{XB}} + V_{BC}(R_{BC}) + V_{XB}(R_{XB}) , \quad \text{(B1)}$$

where $\mu_{BC} = m_B m_C/(m_B+m_C)$ and $\mu_{XB} = m_X m_B/(m_X+m_B)$ are the reduced masses for diatomics BC and XB, respectively. The Hamiltonian (B1) is segregated in the following manner:

$$H = H_0 + V , \quad \text{(B2a)}$$

with

$$H_0 = -\frac{\hbar^2}{2\mu_{BC}}\frac{\partial^2}{\partial R^2_{BC}} - \frac{\hbar^2}{2\mu_{XB}}\frac{\partial^2}{\partial R^2_{XB}} + V_{BC}(R_{BC}) + V_{XB}(R_{XB}) \quad \text{(B2b)}$$

and

$$V = \frac{\hbar^2}{m_B}\frac{\partial^2}{\partial R_{BC}\partial R_{XB}} . \quad \text{(B2c)}$$

The zero-order Hamiltonian (B2b) is now separable in the two coordinates and its spectrum consists of discrete and continuum wavefunctions of the form

$$\langle R_{BC}, R_{XB}|nl\rangle = \chi_n(R_{BC})\phi_l(R_{XB}) , \quad \text{(B3a)}$$

$$\langle R_{BC}, R_{XB}|n\epsilon\rangle = \chi_n(R_{BC})\phi_\epsilon(R_{XB}) , \quad \text{(B3b)}$$

where n denotes the discrete vibrational quantum number of the BC bond, l is the discrete vibrational quantum number of the BX bond, and ϵ designates the relative kinetic energy between X and B. The coupling between discrete and continuum "zero-order" states is now

$$V^{d-c}_{nl,n'\epsilon} = \frac{\hbar^2}{m_B}\langle n|(\partial/\partial R_{BC})|n'\rangle\langle l|(\partial/\partial R_{XB}|\epsilon\rangle . \quad \text{(B4)}$$

Using the relationships

$$\langle n|(\partial/\partial R_{BC})|n'\rangle = \langle n|(\partial V_{BC}/\partial R_{BC})|n'\rangle/(E_n - E_{n'}) , \quad \text{(B5a)}$$

$$\langle l|(\partial/\partial R_{XB})|\epsilon\rangle = \langle l|(\partial V_{XB}/\partial R_{XB})|\epsilon\rangle/(E_l - \epsilon) , \quad \text{(B5b)}$$

and the integrals (A10a), (A10b), and (A12) we obtain for the potentials given in Eqs. (2a) and (3) (i.e., an harmonic oscillator potential for the BC bond and a Morse potential for the XB bond) the result (on the energy shell)

$$V^{d-c}_{nl,n'\epsilon} = (\hbar\omega_{BC}\alpha_{XB}\bar{K}_{XB}/2m_B)(\hbar\mu_{BC}/2\omega_{BC})^{1/2}n^{1/2}$$
$$\times\left[(1/2D_{XB})\sinh(2\pi\bar{\theta}_\epsilon)\frac{(2\bar{K}_{XB}-2l-1)^{1/2}}{l!\,\Gamma(2\bar{K}_{XB}-l)}\right]^{1/2}\frac{|\Gamma(1/2+\bar{K}_{XB}-i\bar{\theta}_\epsilon)|}{[\cos^2(\pi\bar{K}_{XB})+\sinh^2(\pi\bar{\theta}_\epsilon)]^{1/2}}\,\delta_{n',n-1} , \quad \text{(B6)}$$

with the definitions

$$\bar{K}_{XB}=(\hbar\alpha_{XB})^{-1}(2\mu_{XB}D_{XB})^{1/2}\ ,\quad \bar{\theta}_{\epsilon}=(\hbar\alpha_{XB})^{-1}(2\mu_{XB}\epsilon)^{1/2}\ . \tag{B7}$$

The quantities $\bar{K}_{XB}$ and $\bar{\theta}_{\epsilon}$ differ from the corresponding ones K_{XB} and θ_{ϵ} defined in Eq. (11c) by the appearance of the reduced mass $\mu_{XB}=m_X m_B/(m_X+m_B)$ instead of $\mu_{X,BC}=m_X(m_B+m_C)/(m_X+m_B+m_C)$. The decay width Γ^0_{nl} without taking into account continuum–continuum interactions is given by

$$\Gamma^0_{nl}=\pi\sum_{n'}|V^{d-c}_{nl,n',\epsilon}|^2=\hbar\omega_{BC}(\pi/8)\bar{m}\,n[(2K_{XB}-2l-1)/l!\,\Gamma(2K_{XB}-l)]$$
$$\times\{\sinh(2\pi\bar{y})/[\cos^2(\pi\bar{K}_{XB})+\sinh^2(\pi\bar{y})]\}\,|\Gamma(\bar{K}_{XB}+1/2-i\bar{y})|^2\ , \tag{B8}$$

where

$$\bar{y}=[\bar{\beta}-(\bar{K}_{XB}-l-1/2)^2]^{1/2}\ , \tag{B9a}$$

$$\bar{\beta}=2\omega_{BC}\mu_{XB}/\alpha^2_{XB}\ , \tag{B9b}$$

$$\bar{m}=\frac{\mu_{BC}\mu_{XB}}{m_B^2}=\frac{m_C m_X}{(m_B+m_C)(m_X+m_B)}\ . \tag{B9c}$$

This result can be compared with Eq. (1) obtained in the coupling scheme of Sec. II. The two formulas look very much similar. We note that they become identical if we replace (m_B+m_C) by m_B everywhere. The validity of the relative coordinates treatment has already been discussed in the literature.[22(a)] In particular, it was shown that the asymptotic behavior of the continuum wavefunction in this representation is not correct and a renormalization procedure should be applied.[22(a)] From the analysis of this section we conclude that the relative coordinates result (B8) and the nuclear diabatic distorted wave result (1) will give similar results only in the limit $m_B \gg m_C$.

APPENDIX C: THEORY OF VIBRATIONAL PREDISSOCIATION

In what follows we shall utilize the theoretical scheme previously developed by Mukamel, Atabek, and Lefebvre and the present authors[13,15,22] which was already applied to atom–diatom scattering[22] as well as to photodissociation and electronic predissociation of linear triatomics.[13,15] The present derivation adopted for the VP problem is somewhat more transparent and clearly established the relation between, "half-collision" process occurring in molecular photofragmentation and the "full collision" process encounterd in conventional scattering theory. The initially prepared state of the system is $|nl\rangle$ at $t=0$ and the probability for VP into the continuum states $\{|n'\epsilon'\rangle\}$ at time t is

$$P_{n'}(t)=(4\pi^2)^{-1}\int d\epsilon'\left|\int_{-\infty}^{\infty}dE\,G^{+}_{n',\epsilon',nl}(E)\exp(-iEt/\hbar)\right|^2\ , \tag{C1}$$

where $G^{+}_{n',\epsilon',nl}$ is the matrix element of the resolvent operator

$$G^{+}(E)=(E^{+}-H)^{-1}\ , \tag{C2}$$

where E^{+} stands for $E+i\eta$, $\eta\to 0^{+}$. Defining the projection operators

$$\hat{P}=|nl\rangle\langle nl|\ ,$$
$$\hat{Q}=\sum_n\int d\epsilon\,|n\epsilon\rangle\langle n\epsilon|=1-\hat{P} \tag{C3}$$

the evaluation of $G^{+}_{n',\epsilon,nl}$ requires the calculation of the operator $\hat{Q}G^{+}\hat{P}$, which can be shown[23] to be of the form

$$\hat{Q}G^{+}\hat{P}=(E^{+}-\hat{Q}H_0\hat{Q})^{-1}\hat{Q}R\hat{P}(E^{+}-H_0-\hat{P}R\hat{P})^{-1}\ , \tag{C4}$$

where R is the so-called level-shift operator, defined by

$$R=V+V(E^{+}-\hat{Q}H\hat{Q})^{-1}V\ , \tag{C5}$$

where we have denoted by V the difference

$$V=H-H_0\ . \tag{C6}$$

The discrete–continuum and the continuum–continuum coupling operators are defined by

$$V^{c-d}=\hat{Q}V\hat{P}=V^{d-c\dagger}\ ,\quad V^{c-c}=\hat{Q}V\hat{Q}\ . \tag{C7}$$

Using Eq. (C4) we obtain for the relevant matrix elements of G^{+}

$$G^{+}_{n',\epsilon',nl}=\frac{\langle n'\epsilon'|\hat{Q}R\hat{P}|nl\rangle}{(E^{+}-E_{n',\epsilon'})(E^{+}-E_{nl}-\Delta_{nl}+i\Gamma_{nl})}\ , \tag{C8}$$

where Δ_{nl} and $(-\Gamma_{nl})$ are, respectively, the real and imaginary parts of the matrix element $\langle nl|\hat{P}R\hat{P}|nl\rangle$. We may now perform the integration in Eq. (C1) by invoking the usual assumptions regarding the weak dependence of R and the negligible effects of the thresholds. The probability distribution is then given by

$$P_{n'}(t)=(\pi/\Gamma_{nl})\,|\langle n'\epsilon'|\hat{Q}R\hat{P}|nl\rangle|^2[1-\exp(-2\Gamma_{nl}t/\hbar)] \tag{C9}$$

and for $t\to\infty$

$$P_{n'}=(\pi/\Gamma_{nl})\,|\langle n'\epsilon'|\hat{Q}R\hat{P}|nl\rangle|^2\ . \tag{C10}$$

We can now separate formally the contribution of the continuum–continuum interaction by defining a transition T^{c-c} operator which acts only in the $\hat{Q}$ subspace

$$T^{c-c}=V^{c-c}+V^{c-c}(E^{+}-\hat{Q}H\hat{Q})^{-1}V^{c-c}\equiv\hat{Q}R\hat{Q}\ . \tag{C11}$$

The operator $\hat{Q}R\hat{P}$ in Eqs. (C9) and (C10) takes the form

$$\hat{Q}R\hat{P}=V^{c-d}+V^{c-c}(E^{+}-\hat{Q}H\hat{Q})^{-1}V^{c-d}\ , \tag{C12}$$

and using the relation[23]

$$(E^{+}-\hat{Q}H\hat{Q})^{-1}=(E^{+}-\hat{Q}H_0\hat{Q})^{-1}$$
$$+(E^{+}-\hat{Q}H\hat{Q})^{-1}V^{c-c}(E^{+}-\hat{Q}H_0\hat{Q})^{-1} \tag{C13}$$

we obtain

$$\hat{Q}R\hat{P}=[1+T^{c-c}(E^{+}-\hat{Q}H_0\hat{Q})^{-1}]\,V^{c-d}\ . \tag{C14}$$

The operator $(E^{+}-\hat{Q}H_0\hat{Q})^{-1}$ is formally written as

$$(E^{+}-\hat{Q}H_0\hat{Q})^{-1}=\mathrm{PP}[(E-\hat{Q}H_0\hat{Q})^{-1}]-i\pi\delta(E-\hat{Q}H_0\hat{Q})\ , \tag{C15}$$

whose PP stands for the principle part distribution. Invoking the first-order K matrix approximation we neglect the principal part on the right-hand side of Eq. (C15), which amounts to the assumption that the coupling varies slowly with energy. Setting $(E^+ - \hat{Q}H_0\hat{Q})^{-1} = -i\pi\delta(E - \hat{Q}H_0\hat{Q})$ in Eq. (C14) results in the following final expression for the probability distribution:

$$P_{n'} = (\pi/\Gamma_{nl})\left|\sum_{n''}(\delta_{n',n''} - i\pi T^{c-c}_{n',n''})V^{c-d}_{n'',nl}\right|^2 . \quad \text{(C16)}$$

This result can be recast in the form

$$P_{n'} = (\pi/\Gamma_{nl})\left|\sum_{n''}\tilde{S}_{n',n''}V^{c-d}_{n'',nl}\right|^2 ,$$

$$\tilde{S} = 1 - i\pi T^{c-c} , \quad \text{(C17)}$$

where $\tilde{S}$ is the scattering matrix for a half-collision. In view of the K matrix approximation invoked here all the matrix elements are evaluated on the energy shell (consequently, the index ϵ has been omitted in these expressions). In a similar way we have

$$\hat{P}R\hat{P} \equiv V^{d-c}(E^+ - \hat{Q}H\hat{Q})^{-1}V^{c-d} . \quad \text{(C18)}$$

To calculate $\Gamma_{nl} = -\mathrm{Im}\langle nl|\hat{P}R\hat{P}|l\rangle$ we utilize the relation[22]

$$(E - \hat{Q}H\hat{Q})^{-1} = (E - \hat{Q}H_0\hat{Q})^{-1} + (E - \hat{Q}H_0\hat{Q})^{-1}T^{c-c}(E - \hat{Q}H_0\hat{Q})^{-1} , \quad \text{(C19)}$$

which results in

$$\hat{P}R\hat{P} = V^{d-c}(E^+ - \hat{Q}H_0\hat{Q})^{-1}[1 + T^{c-c}(E^+ - \hat{Q}H_0\hat{Q})^{-1}]V^{c-d} . \quad \text{(C20)}$$

Thus, Γ_{nl} is given by [using again $(E^+ - \hat{Q}H_0\hat{Q})^{-1} = -\pi\delta(E - \hat{Q}H_0\hat{Q})$]

$$\Gamma_{nl} = \pi\,\mathrm{Re}\left[\sum_{n',n''} V^{d-c}_{nl,n'}(\delta_{n',n''} - i\pi T^{c-c}_{n',n''})V^{c-d}_{nl,n''}\right] . \quad \text{(C21)}$$

Defining

$$F^{c-c} = 1 - i\pi T^{c-c} \quad \text{(C22)}$$

we note from the definition of T^{c-c} that (neglecting again the principal part integrals)

$$T^{c-c} = V^{c-c}F^{c-c} \quad \text{(C23)}$$

and so

$$F^{c-c} = 1 - i\pi V^{c-c}F^{c-c} . \quad \text{(C24)}$$

The sum of the final probabilities is then

$$\sum_{n'} P_{n'} = \frac{(F^{c-c}V^{c-d})^+(F^{c-c}V^{c-d})}{\mathrm{Re}(V^{d-c}F^{c-c}V^{c-d})} . \quad \text{(C25)}$$

Multiplying now Eq. (C24) by $F^{c-c\dagger}$ from the left we have

$$F^{c-c\dagger}F^{c-c} = F^{c-c\dagger} - iF^{c-c\dagger}V^{c-c}F^{c-c} \quad \text{(C26)}$$

and using the complex conjugate of Eq. (C24) on the right-hand side of Eq. (C26) we obtain

$$F^{c-c\dagger}F^{c-c} = \mathrm{Re}F^{c-c} , \quad \text{(C27)}$$

and therefore replacing Eq. (C27) into (C25) we obtain

$$\sum_{n'} P_{n'} = 1 . \quad \text{(C28)}$$

We now consider briefly the relation of these results with those of conventional scattering. Along the same lines we can calculate the transition probabilities in a collision between X and the molecule BC. Assuming the system to be at $t = -\infty$ in the state $|n, \epsilon\rangle$ the probability for the system to be in the state $|n', \epsilon'\rangle$ with the same total energy at time $t = +\infty$ is given by

$$P_{n\to n'}(E) = |S_{nn'}(E)|^2 , \quad \text{(C29)}$$

where S is the scattering matrix defined by

$$S = 1 - 2i\pi T , \quad \text{(C30)}$$

with

$$T = V + VG^+V . \quad \text{(C31)}$$

Two differences between the VP process and the full-collision process should be noted. First, the $\tilde{S}$ matrix for half-collision [Eq. (C17)] evaluated on the energy shell differs from the S matrix for the full collision [Eq. (C30)], the former involving $-i\pi T^{c-c}$, while the latter contains $-2i\pi T$. Second, we note that T for the scattering problem now operates in the whole space, while T^{c-c} for the VP half-collision process is a similar operator in the Q subspace only.

[1] See for example (a) S. E. Novick, K. C. Janda, S. L. Holmgren, M. Waldman, and W. Klemperer, J. Chem. Phys. **65**, 1114 (1976) and references cited therein; (b) W. Klemperer Ber. Bunsenges. Phys. Chem. **78**, 128 (1974); (c) T. R. Dyke, G. R. Tomasevich, W. Klemperer, and W. E. Falconer, J. Chem. Phys. **57**, 2277 (1972); (d) T. R. Dyke, B. J. Howard, and W. Klemperer, J. Chem. Phys. **56**, 2442 (1972).

[2] In an electronically excited state of a van der Waals molecule, say X•••B–C is a normal diatomic and X a rare-gas atom, other nonradiative decay channels may compete with the VP process. If the electronically excited state of BC can decay via electronic predissociation, the attachment of a rare-gas atom may result in enhancement of the electronic predissociation process reminiscent of collision-induced predissociation.[3] This enhanced electronic predissociation can provide a parallel decay channel of the electronically–vibrationally excited state and does not modify the features of the VP process, which we consider in the present work.

[3] M. Robinson, B. Garetz, and J. I. Steinfeld, J. Chem. Phys. **60**, 3082 (1974).

[4] (a) R. E. Smalley, D. H. Levy, and L. Wharton, J. Chem. Phys. **64**, 3266 (1976); (b) M. S. Kim, R. E. Smalley, L. Wharton, and D. H. Levy, J. Chem. Phys. **65**, 1216 (1976); (c) D. H. Levy (private communication); (d) R. E. Smalley, L. Wharton, and D. H. Levy, J. Chem. Phys. **66**, 2750 (1977).

[5] N. Rosen, J. Chem. Phys. **1**, 319 (1933).

[6] J. A. Beswick and J. Jortner, Chem. Phys. Lett. **49**, 13 (1977).

[7] D. Secrest and W. Eastes, J. Chem. Phys. **56**, 2502 (1972).

[8] D. Rapp and T. E. Sharp, J. Chem. Phys. **38**, 2641 (1963).

[9] F. Mies, J. Chem. Phys. **40**, 523 (1964).

[10] A. F. Devonshire, Proc. R. Soc. (London) Ser. A **158**, 269 (1937).

[11] For the sake of simplicity we shall consider a molecule at $T = 0$, where only the $|g; n = 0, l = 0\rangle$ state is thermally populated.

[12] U. Fano, Phys. Rev. **124**, 1866 (1961).

[13] (a) S. Mukamel, Ph.D. thesis, Tel-Aviv University (1975); (b) S. Mukamel and J. Jortner, J. Chem. Phys. **65**, 3735 (1976).

[14]J. Jackson and N. F. Mott, Proc. R. Soc. (London) Ser. A **137**, 703 (1932).
[15]O. Atabek, J. A. Beswick, R. Lefebvre, S. Mukamel, and J. Jortner, J. Chem. Phys. **65**, 4035 (1976).
[16]M. Abramowitz and I. A. Stegun, *Handbook of Mathematic Functions* (National Bureau of Standards, Washington, 1965).
[17]G. Herzberg, *Spectra of Diatomic Molecules* (Van Nostrand, New York, 1966).
[18](a) J. A. Beswick and R. Lefebvre, Mol. Phys. **23**, 1223 (1972); (b) A. Nitzan, J. Jortner, and B. Berne, Mol. Phys. **26**, 281 (1973).
[19]D. A. Dixon and D. R. Herschbach, Ber. Bunsenges. Phys. Chem. **81**, 145 (1977).
[20]J. A. Beswick and J. Jortner, J. Chem. Phys. (in press).
[21](a) M. S. Child, Faraday Discuss. Chem. Soc. **62**, 307 (1976); (b) C. J. Ashton, Ph.D. thesis, Oxford University (1977); (c) G. Ewing, "The Role of van der Waals Molecules in Vibrational Relaxation Processes" (to be published). We are grateful to Professor Ewing for prepublication information.
[22](a) O. Atabek, J. A. Beswick, and R. Lefebvre, Chem. Phys. Lett. **32**, 28 (1975); (b) **33**, 228 (1975); (c) O. Atabek, J. A. Beswick, R. Lefebvre, S. Mukamel, and J. Jortner, Mol. Phys. **31**, 1 (1976).
[23]L. Mower, Phys. Rev. 142, 799 (1966).